

A Low-rank Augmented Lagrangian Method for Polyhedral-SDP and Moment-SOS Relaxations of Polynomial Optimization

Di Hou*, Tianyun Tang† Kim-Chuan Toh‡

August 29, 2025

Abstract

Polynomial optimization problems (POPs) can be reformulated as geometric convex conic programs, as shown by Kim, Kojima, and Toh (SIOPT 30:1251–1273, 2020), though such formulations remain NP-hard. In this work, we prove that several well-known relaxations can be unified under a common polyhedral-SDP framework, which arises by approximating the intractable cone by tractable intersections of polyhedral cones with the positive semidefinite matrix cone. Although effective in providing tight lower bounds, these relaxations become computationally expensive as the number of variables and constraints grows at the rate of $\Omega(n^{2\tau})$ with the relaxation order τ . To address this challenge, we propose RiNNAL-POP, a low-rank augmented Lagrangian method (ALM) tailored to solve large-scale polyhedral-SDP relaxations of POPs. To efficiently handle the $\Omega(n^{2\tau})$ nonnegativity and consistency constraints, we design a tailored projection scheme whose computational cost scales linearly with the number of variables. In addition, we identify a hidden facial structure in the polyhedral-SDP relaxation, which enables us to eliminate a large number of linear constraints by restricting the matrix variable to affine subspaces corresponding to exposed faces of the semidefinite cone. The latter enables us to efficiently solve the factorized ALM subproblems over the affine subspaces. At each ALM iteration, we additionally carry out a single projected gradient step with respect to the original matrix variable to automatically adjust the rank and escape from spurious local minima when necessary. We also extend our RiNNAL-POP algorithmic framework to solve moment-SOS relaxations of POPs. Extensive numerical experiments on various benchmark problems demonstrate the robustness and efficiency of RiNNAL-POP in solving large-scale polyhedral-SDP relaxations.

keywords: semidefinite programming, augmented Lagrangian, polynomial optimization

Mathematics subject classification: 90C22, 90C23, 90C25

*Department of Mathematics, National University of Singapore, Singapore 119076 (dihou@u.nus.edu).

†Institute of Operations Research and Analytics, National University of Singapore, Singapore 119076 (ttang@u.nus.edu).

‡Department of Mathematics, and Institute of Operations Research and Analytics, National University of Singapore, Singapore 119076 (mattohkc@nus.edu.sg). The research of this author is supported by the Ministry of Education, Singapore, under its Academic Research Fund Tier 3 grant call (MOE-2019-T3-1-010).

1 Introduction

1.1 Polynomial optimization

In this paper, we consider the following polynomial optimization problem:

$$\zeta^* = \min \left\{ f_0(w) \mid f_i(w) = 0, i \in [m], w \in D \right\}, \quad (\text{POP})$$

where $D \subseteq \mathbb{R}^n$ is a cone and each $f_i(w)$ is a real-valued multivariate polynomial. (POP) provides a unified framework for nonconvex polynomial optimization: taking $D = \mathbb{R}^n$ recovers equality-constrained problems, taking $D = \mathbb{R}_+^n$ recovers nonnegatively-constrained problems, and as we will show in Subsection 2.1, general inequality-constrained problems can be handled by introducing standard or squared-slack variables.

POPs arise frequently in combinatorial optimization, control theory, signal processing, and engineering design. Unfortunately, they are NP-hard to solve in general. To address this challenge, various convex reformulations have been proposed to approximate their global minimizers [7, 21, 23].

In the next subsection, we present a unified convex conic reformulation of (POP), which encompasses both completely positive programming (CPP) and positive semidefinite programming (SDP). To keep the presentation concise, we focus mainly on purely conic domains, in particular the nonnegative orthant $D = \mathbb{R}_+^n$ and the Euclidean space $D = \mathbb{R}^n$. But we should emphasize that the theoretical analysis (and the algorithm introduced in Section 3) also applies to relaxations of (POP) even when D is a general semialgebraic-conic domain (cf. [21]).

1.2 Convex conic reformulation

To derive a tractable convex reformulation of the nonconvex problem (POP), we lift it into a higher-dimensional matrix space in three steps: (i) homogenize all polynomials to a common even degree, (ii) introduce a matrix variable whose entries collect all monomials so that each polynomial constraint becomes linear, and (iii) relax by dropping the rank-one requirement and replacing the resulting set of matrices by its convex hull. Under mild geometric conditions, the resulting formulation is equivalent to the original problem.

Homogenization. For any positive integer $\tau \geq \max\{\lceil \deg f_i/2 \rceil \mid i = 0, \dots, m\}$, problem (POP) is equivalent to its degree- 2τ homogeneous form:

$$\zeta^* = \min \left\{ \bar{f}_0(x) \mid \bar{f}_i(x) = 0, i \in [m], x_0 = 1, x = (x_0, w) \in \overline{D} \right\}, \quad (1)$$

where $\overline{D} := \mathbb{R}_+ \times D \subseteq \mathbb{R}^{n+1}$ and \bar{f}_i denotes the degree- 2τ homogenization of f_i (see the notation in (5) of Subsection 1.8).

Lifting. Let $\mathcal{A}_\tau = \{\alpha = (\alpha_0, \dots, \alpha_n) \in \mathbb{N}^{n+1} \mid |\alpha| = \tau\}$ be the set of all degree- τ monomial exponents in \mathbb{R}^{n+1} . For any exponent $\alpha \in \mathbb{N}^{n+1}$, and $x = (x_0; x_1; \dots; x_n) \in \mathbb{R}^{n+1}$, we define $x^\alpha = x_0^{\alpha_0} x_1^{\alpha_1} \cdots x_n^{\alpha_n}$. Choose a subset $\mathcal{A} \subseteq \mathcal{A}_\tau$ so that $\mathcal{A} \times \mathcal{A}$ contains every monomial exponents appearing in $\bar{f}_i(x)$ for $i = 0, \dots, m$. Define $u^\mathcal{A}(x) = (x^\alpha)_{\alpha \in \mathcal{A}}$ as the column

vector of monomial basis with exponents in \mathcal{A} . Let $\mathbb{S}^{\mathcal{A}}$ be the set of symmetric matrices with rows and columns indexed by \mathcal{A} . Then each $\bar{f}_i(x)$ can be written as

$$\bar{f}_i(x) = \left\langle Q^i, u^{\mathcal{A}}(x) (u^{\mathcal{A}}(x))^{\top} \right\rangle \text{ for some } Q^i \in \mathbb{S}^{\mathcal{A}}.$$

Consequently, problem (1) is equivalent to the nonconvex conic program

$$(1) \equiv \text{COP}(K \cap J) : \quad \zeta^* = \min \left\{ \langle Q^0, X \rangle \mid X \in K \cap J, \langle H^0, X \rangle = 1 \right\}, \quad (2)$$

where $H^0 \in \mathbb{S}^{\mathcal{A}}$ has zero entries everywhere except in the row and column indexed by the exponent $e_1^{\tau} := (\tau, 0, \dots, 0) \in \mathcal{A}$ with $H_{e_1^{\tau}, e_1^{\tau}}^0 = 1$, and

$$K = \left\{ u^{\mathcal{A}}(x) (u^{\mathcal{A}}(x))^{\top} \mid x \in \overline{D} \right\}, \quad J = \left\{ X \in \text{co}(K) \mid \langle Q^i, X \rangle = 0 \ \forall i \in [m] \right\}. \quad (3)$$

In the above, $\text{co}(K)$ denotes the convex hull of K .

Convex relaxation. Since K is generally nonconvex, solving $\text{COP}(K \cap J)$ directly is difficult. Instead, we consider the convex relaxation problem over the convex set J :

$$\text{COP}(J) : \quad \zeta^J = \min \left\{ \langle Q^0, X \rangle \mid X \in J, \langle H^0, X \rangle = 1 \right\}. \quad (4)$$

This relaxation is not only convex, but under appropriate conditions, it is also tight, that is, it yields the same optimal value as the original nonconvex problem $\text{COP}(K \cap J)$ (2). The following result provides sufficient conditions for this equivalence (see [21, Theorem 3.1] and [1, Corollary 2.2] for details).

Theorem 1. *Suppose the following conditions hold: (A) K is a nonempty cone in $\mathbb{S}^{\mathcal{A}}$; (B) J satisfies $\text{co}(K \cap J) = J$. Then*

$$-\infty < \zeta^J < \infty \iff -\infty < \zeta^J = \zeta^* < \infty.$$

Remark 1. *The geometric condition $\text{co}(K \cap J) = J$ plays a crucial role in ensuring the exactness of the convex reformulation. This condition has been further studied in [1, 21], where its implications and sufficient conditions are examined in detail. In particular, a sufficient condition for Condition (B) to hold is that J is a face of $\text{co}(K)$.*

Remark 2. *When $\tau = 1$, $\mathcal{A} = \mathcal{A}_1$ and $u(x) = (x_0; \dots; x_n)$, the convex conic reformulation $\text{COP}(J)$ specializes to two well-known cases, depending on the choice of D :*

$$\begin{aligned} D = \mathbb{R}^n &\implies \overline{D} = \mathbb{R}_+ \times \mathbb{R}^n \implies \text{co}(K) = \mathbb{S}_+^{n+1}, & (SDP) \\ D = \mathbb{R}_+^n &\implies \overline{D} = \mathbb{R}_+^{n+1} \implies \text{co}(K) = \text{CPP}^{n+1}, & (CPP) \end{aligned}$$

where $\text{CPP}^{n+1} = \text{co} \{ xx^{\top} \mid x \in \mathbb{R}_+^{n+1} \}$ is the cone of completely positive matrices [3].

1.3 Polyhedral-SDP relaxation

Although $\text{COP}(J)$ serves as a convex reformulation of the original nonconvex polynomial optimization (POP), it may still be intractable because $\text{co}(K)$ can be very complex, where K is defined in (3). For example, testing membership in the cone CPP^{n+1} is NP-hard in general [8]. In this subsection, we introduce tractable relaxations of $\text{COP}(J)$ that yield computationally tractable lower bounds for ζ^* .

To obtain a tractable approximation, we replace $\text{co}(K)$ by the intersection of three cones: the positive semidefinite (PSD) cone $\mathbb{S}_+^{\mathcal{A}}$, a problem-dependent polyhedral cone $\mathcal{P}^{\mathcal{A}} \subseteq \mathbb{S}^{\mathcal{A}}$, and the consistency cone:

$$\mathcal{L}^{\mathcal{A}} = \left\{ X \in \mathbb{S}^{\mathcal{A}} \mid X_{\alpha, \beta} = X_{\gamma, \delta} \text{ if } \alpha + \beta = \gamma + \delta \right\}.$$

The equality constraints in $\mathcal{L}^{\mathcal{A}}$ are generated from the fact that $x^{\alpha+\beta} = x^{\gamma+\delta}$ if $\alpha + \beta = \gamma + \delta$.

As we shall show in Section 2.3, many of the equality constraints defining J exhibit a facial structure and can be compactly written as $AX = 0$ for some full-row-rank matrix $A \in \mathbb{R}^{m \times \mathcal{A}}$. In this paper, we exploit this structure and consider the following polyhedral-SDP relaxation:

$$\zeta^* \geq \zeta^{\text{relax}} = \min \left\{ \langle Q^0, X \rangle \mid \begin{array}{l} \langle H^0, X \rangle = 1, \quad AX = 0, \quad \langle Q^i, X \rangle = 0 \ \forall i \in [\ell], \\ X \in \mathbb{S}_+^{\mathcal{A}} \cap \mathcal{P}^{\mathcal{A}} \cap \mathcal{L}^{\mathcal{A}} \end{array} \right\}. \quad (\text{P})$$

The integer τ such that $\mathcal{A} \subseteq \mathcal{A}_\tau$ is called the relaxation order. This formulation covers a range of convex relaxations—for example, taking

$$\begin{aligned} (\text{SDP}) \quad \text{co}(K) = \mathbb{S}_+^{n+1} \quad &\implies \mathcal{P}^{\mathcal{A}} = \mathbb{S}^{\mathcal{A}}, \\ (\text{DNN}) \quad \text{co}(K) = \text{CPP}^{n+1} \quad &\implies \mathcal{P}^{\mathcal{A}} = \mathcal{N}^{\mathcal{A}}, \end{aligned}$$

yields the standard SDP and doubly-nonnegative (DNN) relaxations, respectively. Here $\mathcal{N}^{\mathcal{A}}$ denotes the cone of nonnegative matrices in $\mathbb{S}^{\mathcal{A}}$. Moreover, by selecting $\mathcal{P}^{\mathcal{A}}$ appropriately, one can obtain relaxations for partial-nonnegativity constraints and other structured domains. If the original polynomial optimization problem (POP) is already homogeneous on a conic domain, one may skip the homogenization step and obtain the relaxation problem (P) without the fixed constraint $\langle H^0, X \rangle = 1$.

To illustrate our framework, we present Example A.1 in Appendix A the quadratic POP from [31, Example 2] as an example to demonstrate its CPP reformulation, DNN relaxation, and facial structure.

1.4 Low-rank augmented Lagrangian method (ALM)

Our main question is how to efficiently solve the relaxed problem (P), which includes both SDP and DNN relaxations as special cases. For the ease of discussion, we focus on the case $\mathcal{A} = \mathcal{A}_\tau$, i.e., the set of all exponents with degrees equal to τ . We identify four major challenges in solving (P):

1. A huge number of $\Omega(mn^\tau + \ell)$ equality constraints;

2. A huge number of $\Omega(n^{2\tau})$ nonnegativity constraints when $D = \mathbb{R}_+^n$;
3. A huge number of $\Omega(n^{2\tau})$ consistency constraints for fixed $\tau \geq 2$;
4. Failure of Slater's condition and strong duality whenever $A \neq 0$.

In this paper, we propose RiNNAL-POP, a low-rank augmented Lagrangian method for solving the general polyhedral-SDP relaxation (P). Our approach builds upon the key ideas of RiNNAL [15] and RiNNAL+ [16], but extends them to handle broader constraint structures and introduces new techniques for exploiting consistency and facial structure within a unified low-rank framework. RiNNAL-POP employs a hybrid strategy that alternates between two phases to efficiently solve the following ALM subproblem:

$$\min \left\{ \begin{array}{l} \langle Q^0, X \rangle + \frac{\sigma}{2} \|\sigma^{-1}y - \mathcal{Q}(X)\|^2 \\ \quad + \frac{\sigma}{2} \|X - \sigma^{-1}W - \Pi_{\mathcal{P}}(X - \sigma^{-1}W)\|^2 \end{array} \middle| \begin{array}{l} AX = 0, X \in \mathbb{S}_+^{\mathcal{A}} \end{array} \right\}, \quad (\text{CVX})$$

where $\sigma > 0$ is the penalty parameter, y and W are the Lagrange multipliers for the constraints $\mathcal{Q}(X) = 0$ and $X \in \mathcal{P}$, respectively, and

$$\mathcal{Q}(X) := \left[\langle Q^1, X \rangle, \dots, \langle Q^\ell, X \rangle \right]^\top, \quad \mathcal{P} := \left\{ X \in \mathcal{P}^{\mathcal{A}} \cap \mathcal{L}^{\mathcal{A}} \mid \langle H^0, X \rangle = 1 \right\}.$$

RiNNAL-POP alternates between a low-rank phase and a convex-lifting phase to solve (CVX) efficiently.

Low-rank phase. Suppose the ALM subproblem (CVX) admits an optimal solution of rank r . To exploit this potential low-rank structure, we apply the Burer–Monteiro (BM) factorization $X = RR^\top$ with $R \in \mathbb{R}^{\mathcal{A} \times r}$, and rewrite (CVX) as the following nonconvex problem:

$$\min \left\{ \begin{array}{l} \langle Q^0, RR^\top \rangle + \frac{\sigma}{2} \|\sigma^{-1}y - \mathcal{Q}(RR^\top)\|^2 \\ \quad + \frac{\sigma}{2} \|RR^\top - \sigma^{-1}W - \Pi_{\mathcal{P}}(RR^\top - \sigma^{-1}W)\|^2 \end{array} \middle| \begin{array}{l} AR = 0, R \in \mathbb{R}^{\mathcal{A} \times r} \end{array} \right\}. \quad (\text{LR})$$

We solve this nonconvex subproblem by using the projected gradient (PG) method on R .

Convex-lifting phase. Since the low-rank subproblem (LR) is nonconvex, the iterate R_t may converge to a suboptimal stationary point. Moreover, the appropriate rank is not known in advance and typically requires careful tuning. To address both issues, the algorithm switches to a convex-lifting phase once R_t reaches near-stationarity. In this phase, we perform a PG step on the original convex problem (CVX), initializing at $X_t = R_t R_t^\top$. We then factorize the updated matrix X_{t+1} to obtain a new iterate R_{t+1} , which serves as the starting point for the next low-rank phase.

This lifting step guarantees a monotonic decrease in the objective value of the ALM subproblem and helps ensuring the convergence to the global optimal solution of the ALM subproblem. Unlike rank-truncation heuristics—which may increase the function value when discarding small singular values—the lifting step automatically adjusts the rank without requiring manual tuning. The idea of using a PG step to automatically update

the rank has been explored in prior works such as [16, 24]. In particular, the numerical experiments in [16] demonstrate that this approach performs remarkably well and typically identifies the correct rank after only a few PG steps. In this paper, we provide a theoretical justification for this phenomenon: we prove that the PG iterates provably identify the optimal rank via manifold identification techniques. Moreover, as we will show in Subsection 3.3, the projection required in each PG step has a closed-form expression, and the projection onto the PSD cone involves only a single eigenvalue decomposition, making each step computationally affordable.

1.5 Summary of our contributions

Our paper’s contributions are summarized as follows:

1. We revisit the polyhedral–SDP relaxation framework of [21] and explicitly provide its equivalence and embedding relationships with RLT, SDP, DNN, and moment–SOS relaxations for general nonconvex polynomial optimization problems with equality and inequality constraints.
2. We leverage the facial structure present in broad families of linear constraints (with RLT and moment–SOS relaxations as two key examples) that expose a face of the semidefinite cone via the equality constraint $AX = 0$. While this structure destroys Slater’s condition and impedes strong duality and numerical stability, our framework overcomes these drawbacks by (1) absorbing the face into the Burer–Monteiro factorization through the smooth subspace constraint $AR = 0$ and (2) fully restoring dual feasibility by explicitly recovering all dual variables from any primal solution.
3. We design RiNNAL-POP, a two-phase augmented Lagrangian method for solving the polyhedral–SDP relaxation (P) of general polynomial optimization problems. In phase one, it solves a low-rank ALM subproblem on the subspace $AR = 0$. In phase two, it applies a single projected gradient update in the full matrix space, where the projection onto the PSD cone with affine constraints admits an explicit closed-form expression. RiNNAL-POP computes the projection onto the intersection of the polyhedral cone and the consistency cone efficiently by averaging identical monomial entries, and enjoys global convergence under mild conditions. Through manifold identification, we prove that the optimal rank is identified automatically, removing the need for manual rank tuning.
4. We extend RiNNAL-POP to solve general τ th-order moment–SOS relaxations by recasting the problem in a split augmented-Lagrangian framework with auxiliary variables for the PSD localization matrices.
5. We conduct extensive computational experiments to evaluate the performance of our RiNNAL-POP algorithm for solving the polyhedral–SDP relaxation (P) and moment–SOS relaxations of various polynomial optimization problems.

1.6 Organization

This paper is organized as follows. In Section 2, we present our unified polyhedral-SDP framework, show how RLT, SDP, DNN, and moment-SOS relaxations fit within this framework, and examine the hidden facial structure. In Section 3, we introduce the augmented Lagrangian framework with the low-rank factorization for solving (P). In Section 4, we present the extension of the algorithm in Section 3 to solve moment-SOS relaxation problems. Section 5 presents several experiments to demonstrate the efficiency and extensibility of the proposed method. Finally, we conclude the paper in Section 6.

1.7 Related works

Interior-point methods (IPMs), as implemented in solvers such as SDPT3 [41], SeDuMi [37], and DSDP [2], can be applied to solve (P). While they are highly effective for small to medium-size SDPs, they scale poorly for large SDP problems, especially for the problem (P) due to their $\mathcal{O}(n^{6\tau})$ per-iteration complexity and high memory demands. To improve scalability, first-order methods based on the alternating direction method of multipliers (ADMM) and the augmented Lagrangian method (ALM) have been widely adopted. For example, SDPNAL+ [38, 45, 46] has shown strong performance for SDP and DNN problems with matrix variables of moderate dimensions. Low-rank solvers that factorize $X = RR^\top$ [12, 27, 40, 43, 44] can be quite effective when the solution is low rank and the number of constraints is moderate. Several low-rank solvers have also been proposed for SDPs [12, 27, 40, 43, 44], based on factorizing the matrix variable as $X = RR^\top$ to reduce dimensionality. These methods are effective when the number of constraints is moderate and the solution is of low rank. However, all the methods mentioned above face significant challenges on large-scale instances—particularly DNN relaxations—due to the rapidly growing number of equality and consistency constraints. Moreover, they may also suffer from the failure of strong duality and do not exploit the possible facial structure of the feasible set.

A closely related line of work is our previous development of RiNNAL [15] and RiNNAL+ [16], which are Riemannian ALM for DNN and SDP-RLT relaxations of mixed-binary quadratic programs. These solvers leverage the low-rank structure of the solution and penalize general inequality and equality constraints while preserving equalities that define the PSD cone’s reduced face and enforce binary constraints in the ALM subproblem. After low-rank factorization, the resulting feasible region of the ALM subproblem becomes an algebraic variety with favorable geometric properties. RiNNAL+ outperforms other solvers on large-scale DNN and SDP-RLT problems, but they are limited to mixed-binary quadratic programs, which do not include the consistency constraints corresponding to \mathcal{L}^A in a general polynomial optimization problem.

1.8 Notation

For any set S , we denote its convex hull by $\text{co}(S)$. Fix a nonnegative integer τ . We define

$$\mathcal{A}_\tau = \{\alpha = (\alpha_0, \alpha_1, \dots, \alpha_n) \in \mathbb{N}^{n+1} : |\alpha| = \alpha_0 + \alpha_1 + \dots + \alpha_n = \tau\}$$

to be the set of all degree- τ monomial exponents in \mathbb{R}^{n+1} with cardinality $\bar{n}_\tau = \binom{n+\tau}{\tau}$. Let $e_1^\tau = (\tau, 0, \dots, 0) \in \mathcal{A}_\tau$ denote the multi-index with $\alpha_0 = \tau$ and all other components

zero. We write $[w]_\tau \in \mathbb{R}^{\bar{n}_\tau}$ for the column vector whose entries are all monomials in $w = (w_1, \dots, w_n)$ of degree $\leq \tau$, arranged in some fixed ordering. Let $p : \mathbb{R}^n \rightarrow \mathbb{R}$ be any polynomial such that $p(w) = \sum_\alpha p_\alpha w^\alpha$. For $\tau \geq \lceil \deg(p)/2 \rceil$, the homogenization of p of degree 2τ is defined by

$$\bar{p}(x) = \bar{p}(x_0, w) = x_0^{2\tau} p\left(\frac{w}{x_0}\right) = \sum_\alpha p_\alpha w^\alpha x_0^{2\tau-|\alpha|}, \quad x = (x_0, w) \in \mathbb{R}^{n+1}. \quad (5)$$

By construction, \bar{p} is homogeneous of degree 2τ , and in particular satisfies $\bar{p}(1, w) = p(w)$. Whenever $\mathcal{A} \subseteq \mathcal{A}_\tau$ is a subset of cardinality $|\mathcal{A}|$, we write

$$\mathbb{S}^{\mathcal{A}} = \mathbb{S}^{|\mathcal{A}|}, \quad \mathbb{R}^{\mathcal{A}} = \mathbb{R}^{|\mathcal{A}|},$$

to emphasize that the matrices in $\mathbb{S}^{|\mathcal{A}|}$ and vectors in $\mathbb{R}^{|\mathcal{A}|}$ are indexed by \mathcal{A} .

2 Polyhedral-SDP relaxations

In this section, we present a unified framework for constructing polyhedral-SDP relaxations of polynomial optimization problems. We begin by showing how any set of polynomial inequalities can be rewritten as equalities via either standard slack variables or squared-slack variables, thereby casting the problem in the general form of (POP) and enabling its direct polyhedral-SDP relaxation (P). We then demonstrate that the classical moment-SOS hierarchy yields precisely the same polyhedral-SDP relaxation, so that each τ th-order moment-SOS program can be interpreted as a facially-exposed SDP of the form (P). Next, we explore how linear constraints of the form $AX = 0$ (arising, for example, from RLT and or moment-SOS relaxations) expose a proper face of the semidefinite cone $\mathbb{S}_+^{\mathcal{A}}$, destroying Slater's condition and giving rise to degeneracies in standard solvers.

2.1 Inequality reformulation via slack variables

Many polynomial optimization problems include inequality constraints. For clarity, we focus here on the case without equality constraints because extending to problems with both equalities and inequalities is straightforward.

Below, we describe two equivalent reformulations that convert each inequality into an equality, so that the problem can be written in the form of (POP) and then relaxed to (P). The overall procedure is summarized in Figure 1. Let $\mathcal{A} \subseteq \mathcal{A}_\tau$ be a monomial index set chosen so that $\mathcal{A} \times \mathcal{A}$ contains all monomial exponents appearing in the homogenized polynomials $\bar{f}_i(x)$ for $i = 0, \dots, m$. We define two extended index sets:

$$\mathcal{A}_1 = (\mathcal{A} \times \{0\}) \cup (e_1^{\tau-1} \times \{1\}), \quad \mathcal{A}_2 = (\mathcal{A} \times \{0\}) \cup (e_1^{\tau-2} \times \{2\}),$$

which correspond, respectively, to the standard-slack and squared-slack formulations. If the same polyhedral set $\mathcal{P}^{\mathcal{A}_1} = \mathcal{P}^{\mathcal{A}_2}$ is imposed in both cases, the resulting polyhedral-SDP relaxations are identical. Verifying this equivalence amounts to a straightforward algebraic check and is omitted for brevity.

In practice, the choice between these two reformulations depends on the domain D . When $D = \mathbb{R}^n$, one typically uses the squared-slack reformulation corresponding to \mathcal{A}_2 ,

which leads directly to an SDP relaxation. When $D = \mathbb{R}_+^n$, the standard-slack reformulation corresponding to \mathcal{A}_1 is more appropriate, yielding a DNN relaxation.

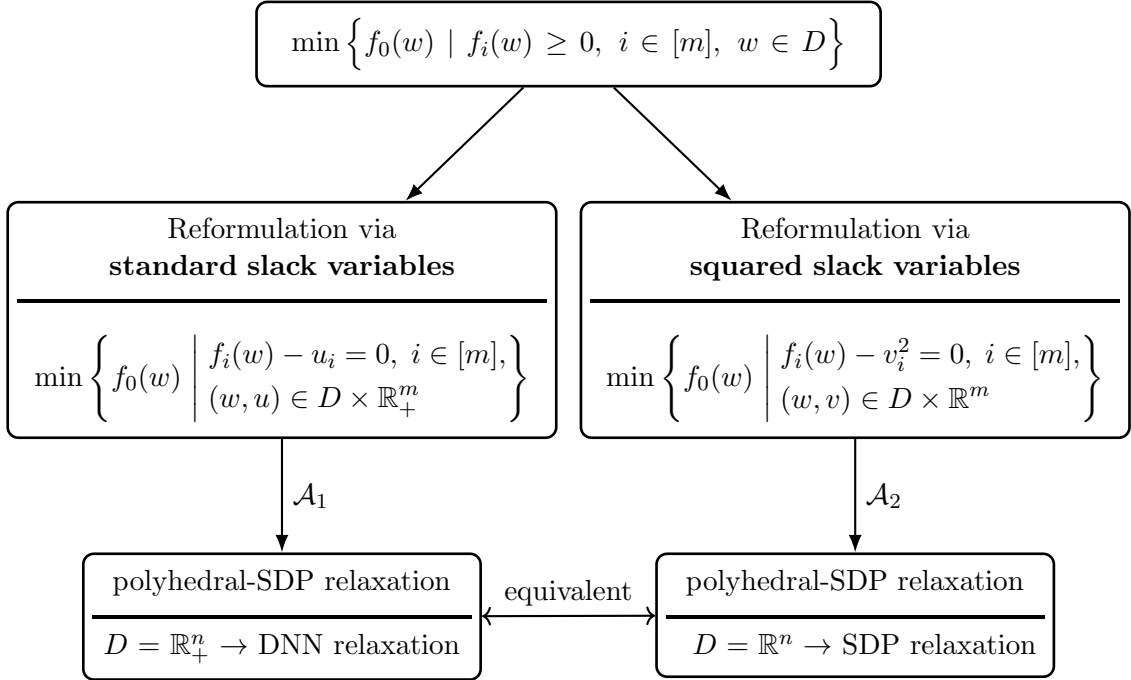


Figure 1: Reformulation and relaxation of polynomial problems with inequality constraints.

2.2 Moment-SOS relaxations

An alternative to the convex-conic reformulation (4) is provided by the moment-SOS hierarchy [23], which approximates the general polynomial optimization problem

$$\min \left\{ f_0(w) \mid g_i(w) = 0, i \in [\ell], h_j(w) \geq 0, j \in [p] \right\} \quad (6)$$

via a sequence of semidefinite relaxations whose optimal values converge to the global optimum under mild assumptions as $\tau \rightarrow \infty$ [23, 42]. Here we assume that D can be expressed entirely by a finite collection of polynomial equalities and inequalities, and hence the condition $w \in D$ is absorbed into the families $\{g_i\}$ and $\{h_j\}$. To set up the τ th-order moment-SOS relaxation, choose

$$\tau \geq \max \left\{ \left\lceil \frac{\deg f_0}{2} \right\rceil, \left\lceil \frac{\deg g_i}{2} \right\rceil (i \in [\ell]), \left\lceil h_j \right\rceil := \left\lceil \frac{\deg h_j}{2} \right\rceil (j \in [p]) \right\}.$$

Then consider the homogenized monomials:

$$x = \begin{bmatrix} x_0 \\ x_1 \\ \vdots \\ x_n \end{bmatrix} = \begin{bmatrix} 1 \\ w_1 \\ \vdots \\ w_n \end{bmatrix}, \quad v(w) := [w]_\tau \in \mathbb{R}^{\bar{n}_\tau}, \quad u(x) := x_0^\tau v \left(\frac{w}{x_0} \right) \in \mathbb{R}^{\bar{n}_\tau}.$$

We refer the readers to Subsection 1.8 for the definition of $[w]_\tau$ and \bar{n}_τ . For example, when $\tau = 2$ and $n = 2$, we have

$$\begin{aligned} x &= [x_0, x_1, x_2]^\top = [1, w_1, w_2]^\top \in \mathbb{R}^3, \\ v(w) &= [1, w_1, w_2, w_1^2, w_1 w_2, w_2^2]^\top \in \mathbb{R}^6, \\ u(x) &= [x_0^2, x_0 x_1, x_0 x_2, x_1^2, x_1 x_2, x_2^2]^\top \in \mathbb{R}^6. \end{aligned}$$

Each equality constraint $g_i(w) = 0$ (with $\deg g_i \leq 2\tau$) generates a collection of redundant equalities. Concretely, for $i \in [\ell]$, one enforces

$$g_i(w) \cdot [w]_{2\tau - \deg g_i} = 0 \iff f_{i,k}(w) = 0, \quad k \in [m_i] \quad (7)$$

so that there are a total of $m = \sum_{i=1}^\ell m_i$ redundant polynomials $f_{i,k}(w)$ with $m_i := \bar{n}_{2\tau - \deg g_i}$, and $i \in [\ell]$. Each of these can be homogenized as

$$\bar{f}_{i,k}(x) = \langle Q^{i,k}, u(x)u(x)^\top \rangle \iff f_{i,k}(w) = \langle Q^{i,k}, v(w)v(w)^\top \rangle$$

with $Q^{i,k} \in \mathbb{S}^{\bar{n}_\tau}$. In the moment relaxation, one replaces

$$u(x)u(x)^\top \mapsto X \in \mathbb{S}_+^{\bar{n}_\tau},$$

and imposes the linear constraints

$$\langle Q^{i,k}, X \rangle = 0, \quad k \in [m_i], \quad i \in [\ell].$$

Each inequality $h_j(w) \geq 0$ (with $\deg(h_j) \leq \tau$) corresponds to a localizing moment matrix:

$$\mathcal{M}_{h_j}(v(w)v(w)^\top) := h_j(w)[w]_{\tau - \lceil h_j \rceil}^\top [w]_{\tau - \lceil h_j \rceil} \succeq 0 \mapsto \mathcal{M}_{h_j}(X) \succeq 0.$$

Combining both types of constraints with $\langle H^0, X \rangle = 1$ (to represent $x_0^{2\tau} = 1$), the τ th-order moment-SOS relaxation of (6) takes the following form, after relabeling $\{Q^{i,k} : k \in [m_i], i \in [l]\}$ as $\{Q^i : i \in [m]\}$:

$$\min \left\{ \langle Q^0, X \rangle \mid \begin{array}{l} \langle H^0, X \rangle = 1, \quad \langle Q^i, X \rangle = 0, \quad i \in [m], \\ \mathcal{M}_{h_j}(X) \succeq 0, \quad j \in [p], \quad X \in \mathbb{S}_+^{\mathcal{A}_\tau} \cap \mathcal{L}^{\mathcal{A}_\tau} \end{array} \right\}. \quad (8)$$

In this subsection, we consider three canonical cases:

- Equality-constrained POP ($D = \mathbb{R}^n$),
- Nonnegativity-constrained POP ($D = \mathbb{R}_+^n$), or
- General inequality-constrained POP ($h_j(w) \geq 0$).

These cases cover many practical applications, and more general domains can be addressed using the reformulation techniques introduced in Subsection 2.1. In each case, the moment-SOS relaxation (8) is equivalent to the polyhedral-SDP relaxation obtained via slack or squared-slack reformulations (as illustrated in Figure 2). Note that the polyhedral-SDP relaxation is tighter than the moment-SOS shown in Figure 2c for the nonnegativity case holds true only when $\tau = 1$. Moreover, the monomial basis \mathcal{A} used in Figure 2d differs for (POP_i) and (POP_i^s) , which corresponds to the reformulation via standard slack variables shown in Figure 1.

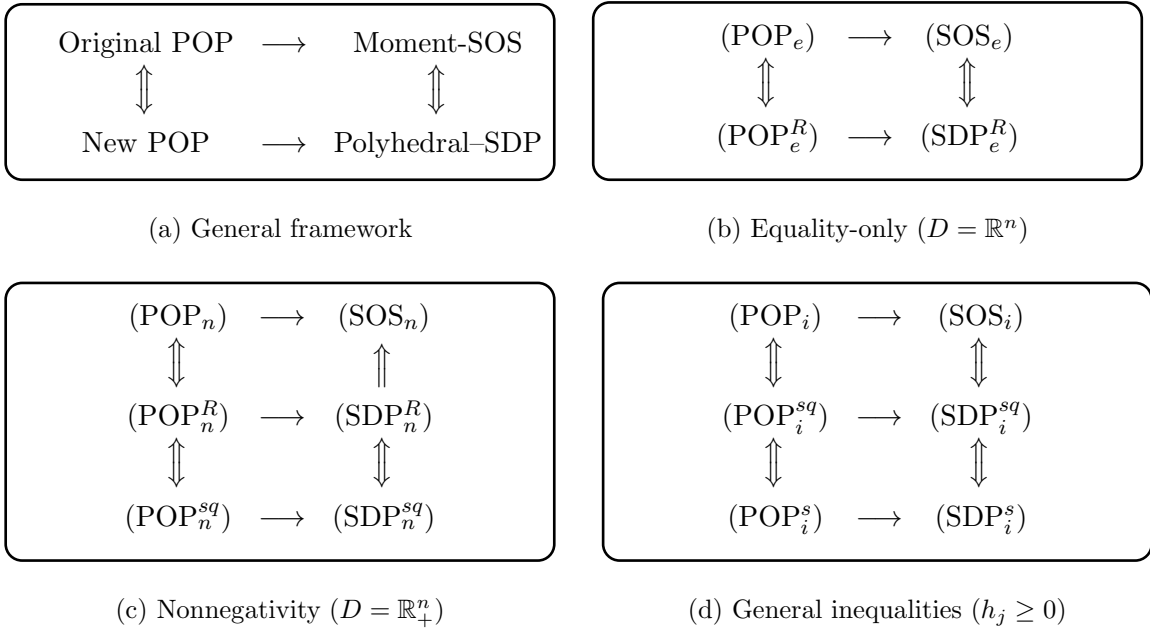


Figure 2: Equivalence between polyhedral-SDP relaxation and moment-SOS relaxation. Note that the polyhedral-SDP relaxation (SDP_n^R) is tighter than the moment-SOS relaxation (SOS_n) in (c) holds true only for the case $\tau = 1$. We refer the reader to the following subsections for the meaning of various problems.

2.2.1 Equality-constrained problem

Consider the polynomial optimization problem with only equality constraints:

$$\min \left\{ f_0(w) \mid g_i(w) = 0, i \in [\ell], w \in \mathbb{R}^n \right\}. \quad (\text{POP}_e)$$

The τ -order moment relaxation of the form (8) is given by

$$\min \left\{ \langle Q^0, X \rangle \mid \langle H^0, X \rangle = 1, \langle Q^i, X \rangle = 0, i \in [m], X \in \mathbb{S}_+^{\mathcal{A}} \cap \mathcal{L}^{\mathcal{A}} \right\}. \quad (\text{SOS}_e)$$

Consider the equivalent problem of (POP_e) with redundant constraints:

$$\min \left\{ f_0(w) \mid f_i(w) = 0, i \in [m], w \in \mathbb{R}^n \right\}, \quad (\text{POP}_e^R)$$

where $f_i(w) = 0$ collects all the equalities generated by (7). Then one can verify that the polyhedral-SDP relaxation of the form (P) for (POP_e^R) coincides with (SOS_e) .

2.2.2 Nonnegativity-constrained problem

Consider the problem with nonnegative variables:

$$\min \left\{ f_0(w) \mid g_i(w) = 0, i \in [\ell], w \in \mathbb{R}_+^n \right\}. \quad (\text{POP}_n)$$

Similarly, the equivalent problem of (POP_n) with redundant constraints is given as:

$$\min \left\{ f_0(w) \mid f_i(w) = 0, i \in [m], w \in \mathbb{R}_+^n \right\}. \quad (\text{POP}_n^R)$$

Its polyhedral-SDP relaxation of the form (P) is given by

$$\min \left\{ \langle Q^0, X \rangle \mid \langle H^0, X \rangle = 1, \langle Q^i, X \rangle = 0, i \in [m], X \in \mathbb{S}_+^{\mathcal{A}} \cap \mathcal{N}^{\mathcal{A}} \cap \mathcal{L}^{\mathcal{A}} \right\}. \quad (\text{SDP}_n^R)$$

We can also replace w in (POP_n) by the product of the squared-variable $s \in \mathbb{R}^n$, yielding

$$\min \left\{ f_0(s \circ s) \mid f_i(s \circ s) = 0, i \in [m], s \in \mathbb{R}^n \right\}. \quad (\text{POP}_n^{sq})$$

By choosing $\bar{\mathcal{A}} = 2\mathcal{A}_\tau$ and enforcing $\mathcal{P}^{\bar{\mathcal{A}}} = \mathcal{N}^{\bar{\mathcal{A}}}$, the polyhedral-SDP relaxation of (POP_n^{sq}) coincides with (SDP_n^R) . In particular, when $\tau = 1$, (SDP_n^R) is tighter than the first-order moment-SOS relaxation of (POP_n) due to the additional nonnegativity constraints.

2.2.3 Inequality-constrained problem

Consider the polynomial optimization problem with only inequality constraints:

$$\min \left\{ f_0(w) \mid h_j(w) \geq 0, j \in [p], w \in \mathbb{R}^n \right\}. \quad (\text{POP}_i)$$

Its τ th-order moment-SOS relaxation is given by

$$\zeta^{(1)} = \min \left\{ \langle Q^0, X \rangle \mid \langle H^0, X \rangle = 1, \mathcal{M}_{h_j}(X) \succeq 0, j \in [p], X \in \mathbb{S}_+^{\mathcal{A}} \cap \mathcal{L}^{\mathcal{A}} \right\}. \quad (\text{SOS}_i)$$

Equivalently, we can introduce squared-slack variables $s_j \in \mathbb{R}$ and rewrite (POP_i) as

$$\min \left\{ f_0(w) \mid h_j(w) - s_j^2 = 0, j \in [p], (w; s) \in \mathbb{R}^{n+m} \right\}. \quad (\text{POP}_i^{sq})$$

Let $\lceil h_j \rceil = \lceil \deg(h_j)/2 \rceil$ for $j \in [p]$. Choose the extended monomial basis

$$v^{\bar{\mathcal{A}}}(w) := \begin{bmatrix} [w]_\tau \\ s_1 [w]_{\tau - \lceil h_1 \rceil} \\ \vdots \\ s_m [w]_{\tau - \lceil h_p \rceil} \end{bmatrix} \in \mathbb{R}^{\bar{\mathcal{A}}}, \quad |\bar{\mathcal{A}}| = \bar{n}_\tau + \underbrace{\sum_{j=1}^p (\tau - \lceil h_j \rceil)}_{:= \bar{p}}$$

and form the lifted moment matrix

$$v^{\bar{\mathcal{A}}}(w) \left(v^{\bar{\mathcal{A}}}(w) \right)^\top \in \mathbb{S}^{\bar{\mathcal{A}}} \quad \mapsto \quad Y := \begin{pmatrix} Y^{11} & Y^{12} \\ Y^{21} & Y^{22} \end{pmatrix} \in \begin{pmatrix} \mathbb{S}^{\bar{n}_\tau} & \mathbb{R}^{\bar{n}_\tau \times \bar{p}} \\ \mathbb{R}^{\bar{p} \times \bar{n}_\tau} & \mathbb{S}^{\bar{p}} \end{pmatrix}.$$

The corresponding polyhedral-SDP relaxation of the form (P) for (POP_i^{sq}) is

$$\zeta^{(2)} = \min \left\{ \langle Q^0, Y^{11} \rangle \mid \langle H^0, Y^{11} \rangle = 1, \mathcal{H}_j(Y) = 0, j \in [p], Y \in \mathbb{S}_+^{\bar{\mathcal{A}}} \cap \mathcal{L}^{\bar{\mathcal{A}}} \right\}, \quad (\text{SDP}_i^{sq})$$

where each linear map $\mathcal{H}_j : \mathbb{S}^{\bar{\mathcal{A}}} \rightarrow \mathbb{R}^{2(\tau - \lceil h_j \rceil)}$ encodes the identity

$$(h_j(w) - s_j^2) [w]_{2(\tau - \lceil h_j \rceil)} = 0 \implies \mathcal{H}_j(Y) = 0.$$

The following theorem establishes the equivalence of (SOS_i) and (SDP_i^{sq}) and derives the reduced formulation.

Theorem 2. (1) The two relaxations (SOS_i) and (SDP_i^{sq}) are equivalent, i.e., $\zeta^{(1)} = \zeta^{(2)}$.
(2) The relaxation (SDP_i^{sq}) is equivalent to the following reduced problem:

$$\zeta^{(2)} = \min \left\{ \langle Q^0, Y^{11} \rangle \mid \begin{array}{l} \langle H^0, Y^{11} \rangle = 1, \mathcal{M}_{h_j}(Y^{11}) - Y_j^{22} = 0, \forall j \in [p], \\ Y^{11} \in \mathbb{S}_+^{\mathcal{A}} \cap \mathcal{L}^{\mathcal{A}}, Y_j^{22} \in \mathbb{S}_+^{\mathcal{A}_j} \cap \mathcal{L}^{\mathcal{A}_j}, \forall j \in [p] \end{array} \right\}, \quad (9)$$

where \mathcal{A}_j is the index set of exponents of $s_j[w]_{\tau-\lceil h_j \rceil}$. Note that (9) is exactly the moment-SOS problem in (SOS_i) by introducing the auxiliary matrices Y_j^{22} , $j \in [p]$.

Proof. (1) First we prove that $\zeta^{(1)} \leq \zeta^{(2)}$. Suppose Y is feasible for (SDP_i^{sq}) . Then $\mathcal{H}_j(Y) = 0$ implies

$$h_j(w)[w]_{\tau-\lceil h_j \rceil}[w]_{\tau-\lceil h_j \rceil}^\top = s_j^2[w]_{\tau-\lceil h_j \rceil}[w]_{\tau-\lceil h_j \rceil}^\top \implies \mathcal{M}_{h_j}(Y^{11}) = Y_j^{22} \succeq 0,$$

where $Y_j^{22} \in \mathbb{S}_+^{\tau-\lceil h_j \rceil}$ denotes the (j, j) -th diagonal block of Y^{22} . Thus, $X = Y^{11}$ is feasible for (SOS_i) with the same objective value, yielding $\zeta^{(1)} \leq \zeta^{(2)}$.

Next we prove that $\zeta^{(1)} \geq \zeta^{(2)}$. Conversely, let X be feasible for (SOS_i) . Define

$$Y := \begin{pmatrix} X & 0_{\bar{n}_\tau \times \bar{p}} \\ 0_{\bar{p} \times \bar{n}_\tau} & \mathcal{M}_h(X) \end{pmatrix}, \quad \mathcal{M}_h(X) := \text{blkdiag}(\mathcal{M}_{h_1}(X), \dots, \mathcal{M}_{h_p}(X)).$$

Then Y is a feasible for (SDP_i^{sq}) with the same objective function, so $\zeta^{(1)} \geq \zeta^{(2)}$.

(2) One may observe that the variable Y^{12} in (SDP_i^{sq}) , which correspond to the monomials in $s_j[w]_{\tau-\lceil h_j \rceil}$ for $j \in [p]$, is not involved in the data matrices in (SDP_i^{sq}) . Thus, we may set Y^{12} and $Y^{21} = (Y^{12})^\top$ to be zero without affecting the optimal value of (SDP_i^{sq}) . Similarly, for the (j, k) -block of Y^{22} , which corresponds to the monomials in $s_j s_k [w]_{\tau-\lceil h_j \rceil} [w]_{\tau-\lceil h_k \rceil}^\top$, is not involved in the data matrices in (SDP_i^{sq}) for $1 \leq j < k \leq p$, and we can set these blocks to zero without affecting the optimal value. Thus we may restrict Y^{22} to be a block diagonal matrix with the (j, j) -th diagonal block Y_j^{22} corresponding to the monomials $(s_j[w]_{\tau-\lceil h_j \rceil})(s_j[w]_{\tau-\lceil h_j \rceil})^\top$ for $j \in [p]$. To summarize, instead of (SDP_i^{sq}) , we can equivalently consider its reduced version:

$$\zeta^{(2)} = \min \left\{ \langle Q^0, Y^{11} \rangle \mid \begin{array}{l} \langle H^0, Y^{11} \rangle = 1, \widehat{\mathcal{H}}_j(Y^{11}, Y_j^{22}) = 0, j \in [p], \\ Y^{11} \in \mathbb{S}_+^{\mathcal{A}} \cap \mathcal{L}^{\mathcal{A}}, Y_j^{22} \in \mathbb{S}_+^{\mathcal{A}_j} \cap \mathcal{L}^{\mathcal{A}_j}, j \in [p] \end{array} \right\},$$

where $\widehat{\mathcal{H}}_j(Y^{11}, Y_j^{22}) = 0$ encodes the equality constraint $(h_j(w) - s_j^2)[w]_{2(\tau-\lceil h_j \rceil)} = 0$ in terms of the new variables Y^{11} and Y_j^{22} . We can readily show that $\widehat{\mathcal{H}}_j(Y^{11}, Y_j^{22}) = 0$ is equivalent to the following condition:

$$\mathcal{M}_{h_j}(Y^{11}) - Y_j^{22} = 0 \quad \forall j \in [p].$$

Thus the problem (9) is equivalent to (SDP_i^{sq}) . ■

2.3 Facial structure

As mentioned in the introduction, in many polynomial optimization relaxations of the form (P), one encounters equality constraints of the form

$$AX = 0, \quad X \succeq 0 \iff \langle A^\top A, X \rangle = 0, \quad X \succeq 0 \iff X \in (A^\top A)^\perp \cap \mathbb{S}_+^{\mathcal{A}}. \quad (10)$$

That is, the feasible set is restricted to a face of the semidefinite cone $\mathbb{S}_+^{\mathcal{A}}$ exposed by the PSD matrix $A^\top A \in \mathbb{S}_+^{\mathcal{A}}$. (Similarly, if (P) has constraints $\langle Q_i, X \rangle = 0$ with $Q_i \succeq 0$ for some $i \in [l]$, we can also replace them by $B_i X = 0$ for some full row-rank matrix B_i satisfying $B_i^\top B_i = Q_i$.) Such ‘‘facial constraints’’ arise naturally in both reformulation-linearization techniques (RLT) [16, 34, 36] and moment-SOS hierarchies [22, 23]. Although facial constraints strengthen the relaxation, they also destroy Slater’s condition, which can make the dual unattainable, and often induce numerical ill-conditioning in SDP solvers [9, 15].

In this subsection, we first analyze the geometric structure of the facial constraints, and then illustrate how these facial constraints naturally arise in (i) RLT relaxations, (ii) moment-SOS relaxations, and (iii) polynomial-optimization problems with binary variables. In Section 3, we explain how our algorithm exploits this facial structure to avoid degeneracy.

Geometric structure. Let $A \in \mathbb{R}^{m \times |\mathcal{A}|}$ be a full-row-rank matrix. Choose any full-row-rank matrix $U \in \mathbb{R}^{(|\mathcal{A}|-m) \times |\mathcal{A}|}$ whose rows form a basis of $\ker(A)$, so that $AU^\top = 0$. Then for every $X \succeq 0$,

$$AX = 0 \iff \langle A^\top A, X \rangle = 0 \iff \exists \Theta \in \mathbb{S}^{|\mathcal{A}|-m} : X = U^\top \Theta U. \quad (11)$$

Hence, the feasible region $\mathbb{S}_+^{\mathcal{A}} \cap \mathcal{F} := \{X \in \mathbb{S}^{\mathcal{A}} \mid AX = 0\}$ is a face of the PSD cone $\mathbb{S}_+^{\mathcal{A}}$, consisting of all PSD matrices whose range is contained in $\ker(A)$. Let $X \in \mathcal{F} \cap \mathbb{S}_+^{\mathcal{A}}$ be any feasible point. By (11), there exists $\Theta \in \mathbb{S}_+^{|\mathcal{A}|-m}$ such that $X = U^\top \Theta U$. The tangent cone to $\mathcal{F} \cap \mathbb{S}_+^{\mathcal{A}}$ at X is then given by

$$T_{\mathcal{F} \cap \mathbb{S}_+^{\mathcal{A}}}(X) = \left\{ H \in \mathbb{S}^{\mathcal{A}} \mid H = U^\top \widehat{H} U, \quad \widehat{H} \in T_{\mathbb{S}_+^{|\mathcal{A}|-m}}(\Theta) \right\}.$$

This follows from the fact that $\mathcal{F} \cap \mathbb{S}_+^{\mathcal{A}}$ is the linear image of the lower-dimensional PSD cone $\mathbb{S}_+^{|\mathcal{A}|-m}$ under the injective linear map $\widehat{H} \mapsto U^\top \widehat{H} U$. Hence, the tangent directions at X correspond exactly to the lifted tangent directions at Θ . The normal cone to $\mathcal{F} \cap \mathbb{S}_+^{\mathcal{A}}$ at X is then given by

$$\begin{aligned} N_{\mathcal{F} \cap \mathbb{S}_+^{\mathcal{A}}}(X) &= \left\{ S \in \mathbb{S}^{\mathcal{A}} \mid USU^\top \in N_{\mathbb{S}_+^{|\mathcal{A}|-m}}(\Theta) \right\} \\ &= \left\{ S \in \mathbb{S}^{\mathcal{A}} \mid -USU^\top \succeq 0, \quad (USU^\top)\Theta = 0 \right\} \\ &= \left\{ S \in \mathbb{S}^{\mathcal{A}} \mid -USU^\top \succeq 0, \quad USX = 0 \right\}. \end{aligned} \quad (12)$$

Reformulation linearization technique (RLT). The convex conic reformulation (4) is equivalent to the original polynomial optimization problem (POP) under suitable conditions. However, its polyhedral-SDP relaxation (P) may remain weak when applied directly

to (POP). To tighten this relaxation, we apply RLT, which multiplies each polynomial constraint by selected monomials to produce new equality constraints. Although these additional equalities are redundant in the original variable space, they become nonredundant in the lifted SDP, further restricting the feasible set and yielding a tighter relaxation.

Although RLT can be applied to both equality and inequality constraints, we focus here on its use for equalities. The treatment of inequalities via slack or squared-slack reformulations follows from Subsection 2.1. Assume that (POP) includes equalities $f_i(w) = 0$ whose homogenized forms $\bar{f}_i(x)$ are linear in $u^A(x)$, i.e.,

$$\bar{f}_i(x) = \langle a_i, u^A(x) \rangle \text{ for some } a_i \in \mathbb{R}^A.$$

Collecting these coefficient vectors into $A := [a_1, \dots, a_m]^\top \in \mathbb{R}^{m \times A}$. We see that $\bar{f}_i(x) = 0$ is equivalent to $A u^A(x) = 0$. Multiplying each equation by the vector $u^A(x)^\top$ yields the RLT-type constraints $AX = 0$, which can be added to (P) to tighten the relaxation. The derivation is summarized in Figure 3.

$$\begin{array}{ccc} \begin{bmatrix} \bar{f}_1(x) \\ \vdots \\ \bar{f}_m(x) \end{bmatrix} = 0 & \iff & \begin{bmatrix} \bar{f}_1(x) \\ \vdots \\ \bar{f}_m(x) \end{bmatrix} (u^A(x))^\top = 0 \\ \uparrow\downarrow & & \uparrow\downarrow \\ A u^A(x) = 0 & \iff & A u^A(x) (u^A(x))^\top = 0 \implies AX = 0. \end{array}$$

Figure 3: Derivation of RLT constraints with facial structure.

Moment-SOS relaxations. When applying the moment-SOS hierarchy to the general POP (6), each equality $g_i(w) = 0$ with $\deg(g_i) \leq \tau$ gives rise to redundant polynomial constraints of the form

$$g_i(w)[w]_{2\tau-\deg(g_i)} = 0,$$

which can be rewritten as

$$(g_i(w)[w]_{\tau-\deg(g_i)}) [w]_\tau^\top = 0 \iff G_i[w]_\tau [w]_\tau^\top = 0$$

where $G_i \in \mathbb{R}^{d_i \times \bar{n}_\tau}$ is the coefficient matrix of the polynomials $g_i(w)[w]_{\tau-\deg(g_i)}$ with respect to the basis $[w]_\tau$, and

$$d_i = \binom{n + \tau - \deg(g_i)}{\tau - \deg(g_i)}.$$

Lifting $[w]_\tau [w]_\tau^\top$ to the matrix variable $X \in \mathbb{S}_+^{\bar{n}_\tau}$ yields the linear constraint

$$G_i X = 0, \quad i = 1, \dots, \ell.$$

Collecting the above constraint matrices into

$$A = \begin{bmatrix} G_1 \\ \vdots \\ G_\ell \end{bmatrix} \implies AX = 0,$$

we see that all equality constraints with $\deg(g_i) \leq \tau$ in the moment–SOS relaxation can be written concisely as $AX = 0$.

We illustrate the procedure in Figure 3 by an example below.

Example 2.1. Consider the nonnegative quadratic programming problem:

$$\min \left\{ w^\top Q w + 2c^\top w \mid a_i^\top w = b_i, i \in [m], w \in \mathbb{R}_+^n \right\}.$$

Set $\tau = 1$ and choose the full degree-1 monomial basis \mathcal{A}_1 . Then

$$u^{\mathcal{A}}(x) = [x_0, x_1, \dots, x_n]^\top = [1, w_1, \dots, w_n]^\top \in \mathbb{R}^{n+1}.$$

By RLT, each linear constraint $a_i^\top w = b_i$ implies

$$[-b_i \ a_i^\top] u^{\mathcal{A}}(x) = 0 \implies [-b_i \ a_i^\top] X = 0.$$

By collecting all m such rows, we define

$$A = \begin{bmatrix} -b_1 & a_1^\top \\ \vdots & \\ -b_m & a_m^\top \end{bmatrix} \in \mathbb{R}^{m \times (n+1)},$$

so that $AX = 0$ enforces all linear equalities in the lifted SDP. The resulting polyhedral-SDP (or moment–SOS) relaxation is

$$\min \left\{ \langle Q^0, X \rangle \mid \langle H^0, X \rangle = 1, AX = 0, X \in \mathbb{S}_+^{n+1} \cap \mathcal{N}^{n+1} \right\},$$

where

$$Q^0 = \begin{bmatrix} 0 & c^\top \\ c & Q \end{bmatrix}, \quad H^0 = \begin{bmatrix} 1 & 0_n^\top \\ 0_n & 0_{n \times n} \end{bmatrix}.$$

A common approach to eliminate the affine constraint $AX = 0$ in the SDP problem is facial reduction [6], which replaces X with a lower-dimensional variable Θ as defined in (11). This method has been applied to specific cases [22, Section 3.2], where the constraints in (POP) are binary, such as $x_i^2 = x_i$ or $x_i^2 = 1$, and facial reduction reduces to removing redundant rows and columns. However, for general problems (POP), this process typically destroys the sparsity of the remaining linear constraints. In the next section, we present a more efficient approach that preserves sparsity while handling affine constraints.

3 Algorithm

In this section, we introduce the proposed method RiNNAL-POP for solving the following general polyhedral-SDP problem:

$$\min \left\{ \langle C, X \rangle \mid \mathcal{Q}(X) = b, X \in \mathcal{F} \cap \mathcal{P} \cap \mathbb{S}_+^n \right\}, \quad (\text{SDP})$$

where $\mathcal{Q} : \mathbb{S}^n \rightarrow \mathbb{R}^d$ is a given linear mapping with $b \in \mathbb{R}^d$, and \mathcal{P} is a polyhedral convex set in \mathbb{S}^n . We assume that \mathcal{F} has the compact form:

$$\mathcal{F} = \{X \in \mathbb{S}^n \mid AX = 0\},$$

where $A \in \mathbb{R}^{m \times n}$ has full row-rank. (SDP) is a generalization of the polyhedral-SDP relaxation (P). In particular, one can take \mathcal{P} as the intersection $\mathcal{P}^A \cap \mathcal{L}^A \cap \{X \in \mathbb{S}^A \mid \langle H^0, X \rangle = 1\}$, i.e., the nonnegativity cone, the consistency cone, and the normalization hyperplane. The basic framework of RiNNAL-POP follows those in [15, 16] that were originally developed to solve SDP-RLT and DNN relaxations of mixed-binary quadratic programs. Here we extend the algorithms in [15, 16] to address the problem (SDP). To apply the augmented Lagrangian framework, we rewrite (SDP) in an equivalent splitting form

$$\min \left\{ \langle C, X \rangle + \delta_{\mathcal{F} \cap \mathbb{S}_+^n}(X) + \delta_{\mathcal{P}}(Y) \mid X - Y = 0, \mathcal{Q}(X) = b \right\}, \quad (13)$$

where δ_C denotes the indicator function of a convex set C . Once we have computed (X^*, Y^*) (and the associated multipliers), we certify its global optimality by checking the following Karush–Kuhn–Tucker (KKT) conditions of (13):

$$\begin{aligned} X - Y = 0, \quad AX = 0, \quad \mathcal{Q}(X) = b, \quad C - W - A^\top U - U^\top A - \mathcal{Q}^*(y) = S, \\ \langle X, S \rangle = 0, \quad X \succeq 0, \quad S \succeq 0, \quad W \in N_{\mathcal{P}}(Y), \quad Y \in \mathcal{P}, \end{aligned} \quad (14)$$

where $U \in \mathbb{R}^{m \times n}$, $W \in \mathbb{R}^{n \times n}$, $y \in \mathbb{R}^d$, and $S \in \mathbb{S}^n$ are the dual variables. Here $N_{\mathcal{P}}(Y)$ denotes the normal cone of the set \mathcal{P} at the point Y . We make the following assumption throughout the paper.

Assumption 1. *Problem (SDP) admits an optimal solution satisfying the KKT conditions (14), and its objective function is bounded from below.*

Remark 3. *Although (10) shows that enforcing three different constraints yields the same primal feasible set, their dual formulations differ. In particular, when $A \neq 0$, expressing the constraint as $\langle Q^i, X \rangle = 0$ or $\langle AA^\top, X \rangle = 0$ exacerbates the failure of Slater’s condition and can enlarge the duality gap. In contrast, the linear form $AX = 0$ produces the smallest duality gap among these alternatives—and under mild regularity conditions attains zero duality gap (see [5, 15, 16]). In Section 3.5, we explain how to recover the corresponding dual multipliers and how to handle the enlarged constraint system efficiently in our algorithm.*

Remark 4. *In (SDP), we enforce the constraint $\langle H^0, X \rangle = 1$ in the set \mathcal{P} rather than the feasible set \mathcal{F} for simplicity of presentation. However, for polyhedral-SDP relaxations of polynomial optimization problems involving mixed-binary constraints (i.e., $x_i \in \{0, 1\}$), it is preferable to include this constraint in \mathcal{F} . This treatment is adopted in [15, 16] and typically leads to a performance improvement of at least 50%.*

3.1 Augmented Lagrangian method

RiNNAL-POP is an augmented Lagrangian method for solving (SDP). The augmented Lagrange function of its equivalent split form (13) is defined by

$$\begin{aligned} L_\sigma(X, Y; y, W) &:= \langle C, X \rangle - \langle y, \mathcal{Q}(X) - b \rangle - \langle W, X - Y \rangle + \frac{\sigma}{2} \|\mathcal{Q}(X) - b\|^2 + \frac{\sigma}{2} \|X - Y\|^2 \\ &= \langle C, X \rangle + \frac{\sigma}{2} \|\mathcal{Q}(X) - b - \sigma^{-1}y\|^2 + \frac{\sigma}{2} \|X - Y - \sigma^{-1}W\|^2 - \frac{1}{2\sigma} \|y\|^2 - \frac{1}{2\sigma} \|W\|^2. \end{aligned}$$

Given the initial penalty parameter $\sigma_0 > 0$, dual variable $y^0 \in \mathbb{R}^d$ and $W^0 \in \mathbb{R}^{n \times n}$, the augmented Lagrangian method performs the following steps at the $(k+1)$ -th iteration:

$$\begin{aligned} (X^{k+1}, Y^{k+1}) &= \arg \min \left\{ L_{\sigma_k}(X, Y; y^k, W^k) : X \in \mathcal{F} \cap \mathbb{S}_+^n, Y \in \mathcal{P} \right\}, \quad (15) \\ y^{k+1} &= y^k - \sigma_k(\mathcal{Q}(X^{k+1}) - b), \\ W^{k+1} &= W^k - \sigma_k(X^{k+1} - Y^{k+1}), \end{aligned}$$

where $\sigma_k \uparrow \sigma_\infty \leq +\infty$ are positive penalty parameters. For a comprehensive discussion on the augmented Lagrangian method applied to convex optimization problems and beyond, see [14, 32, 35]. Let \tilde{y} and $\tilde{W} \in \mathbb{S}^n$ be fixed. The inner problem (15) can be expressed as:

$$\min \left\{ L_\sigma(X, Y; \tilde{y}, \tilde{W}) : X \in \mathcal{F} \cap \mathbb{S}_+^n, Y \in \mathcal{P} \right\}. \quad (16)$$

In (16), we can first minimize with respect to $Y \in \mathcal{P}$ to get the following convex optimization problem related only to X :

$$\min \left\{ \begin{array}{l} \phi(X) := \langle C, X \rangle + \frac{\sigma}{2} \|\sigma^{-1}y - (\mathcal{Q}(X) - b)\|^2 \\ \quad + \frac{\sigma}{2} \|X - \sigma^{-1}W - \Pi_{\mathcal{P}}(X - \sigma^{-1}W)\|^2 \end{array} \middle| X \in \mathcal{F} \cap \mathbb{S}_+^n \right\}, \quad (\text{CVX})$$

Once we obtain the optimal solution \tilde{X} of (CVX), we can recover the optimal solution $\tilde{Y} = \Pi_{\mathcal{P}}(\tilde{X} - \sigma^{-1}\tilde{W})$. The ALM framework for solving (13) is summarized in Algorithm 1, where X^{k+1} is obtained by the factorization described in the next subsection.

3.2 Low-Rank Phase

In this phase, we follow the approach introduced in [15, 16] to solve (CVX). Let $\sigma > 0$, $y \in \mathbb{R}^d$, and $W \in \mathbb{R}^{n \times n}$ be fixed, and suppose that the subproblem (CVX) admits an optimal solution of rank $r > 0$. By the Burer–Monteiro (BM) factorization, any rank- r solution can be written as

$$X \in \mathcal{F} \cap \mathbb{S}_+^n \implies X = RR^\top \text{ for some } R \in \mathbb{R}^{n \times r}.$$

The crucial property

$$AX = 0 \iff A(RR^\top) = 0 \iff AR = 0 \quad (17)$$

Algorithm 1 The RiNNAL-POP method

- 1: **Parameters:** Given $\sigma_0 > 0$, integer $r_0 > 0$, initial point $R^0 \in \mathbb{R}^{n \times r_0}$.
- 2: $k \leftarrow 0$, $i \leftarrow 0$, $y^0 = 0_d$, $W^0 = 0_{n \times n}$.
- 3: **while** (SDP) is not solved to required accuracy **do**
- 4: **while** (CVX) is not solved to required accuracy **do**
- 5: Obtain R^{i+1} by solving (LR) satisfying (18).
- 6: Obtain $\widehat{X}^{i+1} = R^{i+1}(R^{i+1})^\top$.
- 7: Obtain X^{i+1} by solving (CVX) via one step of PG satisfying (20).
- 8: Obtain R^{i+1} from the eigenvalue decomposition of X^{i+1} .
- 9: **end while**
- 10: $X^{k+1} = X^i$.
- 11: $Y^{k+1} = \Pi_P(X^{k+1} - \sigma^{-1}W^k)$.
- 12: $y^{k+1} = y^k - \sigma_k(\mathcal{Q}(X^{k+1}) - b)$.
- 13: $W^{k+1} = W^k - \sigma_k(X^{k+1} - Y^{k+1})$.
- 14: Update σ_k .
- 15: $k \leftarrow k + 1$, $i \leftarrow 0$.
- 16: **end while**

shows that enforcing $X \in \mathcal{F}$ (i.e. $AX = 0$) is equivalent to the affine constraint $AR = 0$ on R . Consequently, the original SDP subproblem (CVX) is equivalent to the following factorized (nonconvex) problem:

$$\min \left\{ f_r(R) := \phi(RR^\top) \mid AR = 0 \right\}, \quad (\text{LR})$$

where the constraint $AR = 0$ defines an affine subspace of dimension $(n - m)r$. In this form, the decision-variable's dimension is reduced from $n \times n$ to $n \times r$, and the number of linear constraints is effectively reduced from the original mn equations on the $n \times n$ matrix variable X to mr equations on R . Thus, one can directly apply any suitable first-order method (for example, projected gradient descent) to (LR) without explicitly handling the full $n \times n$ PSD cone. In practice, this reduction in both the dimension and number of constraints often yields substantial savings in memory and per-iteration cost. The reduction enabled by the crucial property (17) is key to the success of our final algorithm RiNNAL-POP.

We impose only the following mild, implementable non-increasing objective condition on the low-rank phase:

$$f_r(R^{i+1}) \leq f_r(R^i) \Leftrightarrow \phi_r(R^{i+1}(R^{i+1})^\top) \leq \phi_r(R^i(R^i)^\top). \quad (18)$$

The subproblem (LR) is nonconvex, so the algorithm must be capable of escaping from saddle points. Moreover, the factorized formulation is equivalent to the original SDP only when the chosen rank exceeds the true optimal rank. To enforce these requirements, we introduce a convex lifting phase that automatically increases r as needed and guarantees a monotonic decrease in the objective value to escape saddle points, thereby ensuring convergence to a global solution.

3.3 Convex lifting phase

In the convex lifting phase, we adopt the strategy proposed in [24] to ensure global convergence of RiNNAL+ while automatically adjusting the rank. Let $\sigma > 0$, $y \in \mathbb{R}^d$, and $W \in \mathbb{R}^{n \times n}$ be fixed. Given any feasible starting point $\widehat{X} \in \mathcal{F} \cap \mathbb{S}_+^n$, we conduct a single projected-gradient step on the SDP-subproblem (CVX):

$$X = \Pi_{\mathcal{F} \cap \mathbb{S}_+^n} \left(\widehat{X} - t \nabla \phi(\widehat{X}) \right) = \arg \min \left\{ \|X - G\|^2 \mid X \in \mathcal{F} \cap \mathbb{S}_+^n \right\}, \quad (19)$$

where $G := \widehat{X} - t \nabla \phi(\widehat{X})$ and $t > 0$ is an appropriate stepsize. One can compute X efficiently in closed form (cf. [16, Lemma 2]):

$$X = \Pi_{\mathbb{S}_+^n} (JGJ), \quad J := I - A^\top (AA^\top)^{-1} A.$$

For the stepsize choices, the only requirement of our framework is that the final stepsize of each ALM subproblem is uniformly bounded and satisfies the following criteria for some given $\delta \in (0, 1)$:

$$\phi(X^{i+1}) \leq \phi(X^i) + \langle \nabla \phi(\widehat{X}^i), X^{i+1} - \widehat{X}^i \rangle + \frac{\delta}{t_i} \|X^{i+1} - \widehat{X}^i\|^2. \quad (20)$$

To ensure that t_i is bounded, we need to specify an upper t_{\max} and a lower bound t_{\min} . It is known that if $\nabla \phi$ is L -Lipschitz continuous, then (20) holds for any $t_i \leq 2\delta/L$, and thus we assign $t_{\min} \leq 2\delta/L$ to ensure that our algorithm is well-defined. Since the convex lifting phase is not the major tool for reducing the objective value, we simply assign a fixed step size $t_i = t$ in our implementation.

This phase offers several advantages:

- Primal feasibility enforcement: a single projection restores primal feasibility of X .
- Convergence guarantee: the projection helps to escape from saddle points in the low-rank phase and yields a monotonic decrease in the objective with a suitably chosen stepsize, thus ensuring global convergence of the ALM subproblem. For a more detailed analysis, see [24].
- Automatic rank selection: the lifting phase automatically identifies a rank r satisfying $r \geq r^*$ to ensure equivalence between the low-rank subproblem (LR) and the SDP-subproblem (CVX), while keeping r as small as possible to minimize memory usage and per-iteration cost. We provide a rigorous theoretical justification for this behavior from the perspective of rank identification in the next subsection.

Together, these properties enable a reliable initialization, provide an accurate rank estimate, and enhance computational efficiency, ultimately ensuring the global convergence of RiNNAL-POP.

3.4 Rank identification

In the convex lifting phase, we use a projected-gradient scheme to solve the augmented Lagrangian subproblem (CVX), which can be equivalently written as

$$\min_X F(X) := \phi(X) + \Psi(X), \quad (\text{CVX})$$

where the function ϕ is lower-bounded, convex, and differentiable with L -Lipschitz continuous gradient, and the function Ψ is convex and has the form

$$\Psi(X) := \delta_{\mathcal{F} \cap \mathbb{S}_+^n}(X), \quad \mathcal{F} = \{X \in \mathbb{S}^n \mid AX = 0\}. \quad (21)$$

Empirically, these projected-gradient iterates very rapidly ‘‘lock on’’ to the true rank of the optimal solution of (CVX), see [16] for numerical comparisons highlighting the advantage of the PG step over adaptive rank-tuning strategies. To explain this behavior rigorously, we establish a finite-step rank identification result: under a standard nondegeneracy condition, the PG iterates lie on the smooth manifold of fixed-rank matrices after finitely many steps. This provides the theoretical justification for the practical efficiency of our convex lifting phase in identifying the true rank of the optimal solution of (CVX).

Before proceeding to the convergence analysis, we introduce the definition of convex partly smooth functions. This concept is based on the notion of a C^2 -manifold, that is, a manifold defined by equations that are twice continuously differentiable.

Definition 1 (Partly smooth [25]). *A convex function Ψ is partly smooth at a point X^* relative to a set \mathcal{M} containing X^* if $\partial\Psi(X^*) \neq \emptyset$ and:*

1. *Around X^* , \mathcal{M} is a C^2 -manifold and $\Psi|_{\mathcal{M}}$ is C^2 .*
2. *The affine span of $\partial\Psi(X)$ is a translate of the normal space to \mathcal{M} at X^* .*
3. *$\partial\Psi$ is continuous at X^* relative to \mathcal{M} .*

Informally, this means that $\Psi|_{\mathcal{M}}$ is smooth at X^* , whereas its value varies sharply in directions departing from \mathcal{M} in a neighborhood of X^* . It is known [25] that for every $X^* \in \mathbb{S}_+^n$, the indicator function $\delta_{\mathbb{S}_+^n}$ is partly smooth at X^* with respect to the manifold

$$\mathcal{M}_+(X^*) := \{Y \in \mathbb{S}_+^n \mid \text{rank}(Y) = \text{rank}(X^*)\}. \quad (22)$$

In the sequel, we extend this partial smoothness result to $\mathcal{F} \cap \mathbb{S}_+^n$, a face of the PSD cone. Note that the standard approach of establishing partial smoothness via transversality cannot be applied here, as the required transversality condition fails to hold. Therefore, we check Definition 1 directly to verify partial smoothness.

Lemma 1 (Partial smoothness of Ψ). *At every $X^* \in \mathcal{F} \cap \mathbb{S}_+^n$, the indicator function $\Psi(X) := \delta_{\mathcal{F} \cap \mathbb{S}_+^n}(X)$ is partly smooth with respect to the manifold*

$$\mathcal{M}_+^{\mathcal{F}}(X^*) := \{Y \in \mathbb{S}_+^n \mid AY = 0, \text{rank}(Y) = \text{rank}(X^*)\}.$$

Proof. We verify partial smoothness by checking the three defining conditions in Definition 1. By (11), there exists a full-row-rank matrix $U \in \mathbb{R}^{(n-m) \times n}$ whose rows form a basis of $\ker(A)$ (hence $AU^\top = 0$). Define the linear map

$$\Phi : \mathbb{S}^{n-m} \rightarrow \mathcal{F}, \quad \Theta \mapsto U^\top \Theta U,$$

which is a bijective. In particular, for every $X \in \mathcal{F} \cap \mathbb{S}_+^n$, there exists a unique $\Theta \in \mathbb{S}_+^{n-m}$ such that

$$X = \Phi(\Theta) = U^\top \Theta U \iff \Theta = \Phi^{-1}(X) = (UU^\top)^{-1}UXU^\top(UU^\top)^{-1}. \quad (23)$$

In the special case $X = X^*$, we write $\Theta^* := \Phi^{-1}(X^*)$, so that $X^* = \Phi(\Theta^*)$. We will make frequent use of this correspondence in the subsequent proof.

(1) By the linear transformation (23), we have

$$\mathcal{M}_+^{\mathcal{F}}(X^*) = \Phi(\mathcal{M}_+(\Theta^*)),$$

where $\mathcal{M}_+(\Theta^*)$ is the fixed-rank PSD manifold in \mathbb{S}^{n-m} defined in (22). Since Φ is a bijective linear map, it restricts to a C^∞ diffeomorphism from $\mathcal{M}_+(\Theta^*)$ onto $\mathcal{M}_+^{\mathcal{F}}(X^*)$. Therefore $\mathcal{M}_+^{\mathcal{F}}(X^*)$ is a smooth embedded submanifold of \mathbb{S}^n . Since $\mathcal{M}_+^{\mathcal{F}}(X^*) \subseteq \mathcal{F} \cap \mathbb{S}_+^n$, the indicator function Ψ is identically zero on $\mathcal{M}_+^{\mathcal{F}}(X^*)$, and is thus smooth when restricted to $\mathcal{M}_+^{\mathcal{F}}(X^*)$.

(2) The subdifferential of Ψ at X^* is given by

$$\partial\Psi(X^*) = N_{\mathcal{F} \cap \mathbb{S}_+^n}(X^*) = \left\{ S \in \mathbb{S}^n \mid -USU^\top \succeq 0, (USU^\top)\Theta^* = 0 \right\}, \quad (24)$$

where we use the expression of the normal cone derived in (12). Using a similar strategy as that in Subsection 2.3, we obtain

$$T_{\mathcal{M}_+^{\mathcal{F}}(X^*)}(X^*) = \left\{ H \in \mathbb{S}^n \mid H = U^\top \hat{H}U, \hat{H} \in T_{\mathcal{M}_+(\Theta^*)}(\Theta^*) \right\},$$

where $\mathcal{M}_+(\Theta^*)$ is defined as in (22). The corresponding normal cone is

$$N_{\mathcal{M}_+^{\mathcal{F}}(X^*)}(X^*) = \left\{ S \in \mathbb{S}^n \mid USU^\top \in N_{\mathcal{M}_+(\Theta^*)}(\Theta^*) \right\} = \left\{ S \in \mathbb{S}^n \mid (USU^\top)\Theta^* = 0 \right\},$$

which coincides with the affine span of $\partial\Psi(X^*)$ in (24).

(3) Since $\delta_{\mathbb{S}_+^{n-m}}(\Theta)$ is continuous at Θ^* relative to $\mathcal{M}_+(\Theta)$, continuity is preserved under the bijection Φ . Indeed,

$$\Phi^*(\partial\Psi(X)) = \left\{ USU^\top \in \mathbb{S}^{n-m} \mid -USU^\top \succeq 0, (USU^\top)\Theta = 0 \right\} = \partial\delta_{\mathbb{S}_+^{n-m}}(\Theta),$$

hence $\partial\Psi(X) = (\Phi^*)^{-1}(\partial\delta_{\mathbb{S}_+^{n-m}}(\Theta))$, which proves the claim.

Having verified conditions (1)–(3), we conclude that $\delta_{\mathcal{F} \cap \mathbb{S}_+^n}$ is partly smooth at X^* relative to $\mathcal{M}_+^{\mathcal{F}}(X^*)$. ■

Now we can leverage tools from partial smoothness and manifold identification to show that our algorithm will find the correct rank for (CVX) that contains a global optimum. The result follows directly from [24] by analogous arguments and is thus omitted.

Theorem 3. Consider (CVX) with Ψ defined in (21). Consider the two sequences of iterates $\{X^i\}$ and $\{\widehat{X}^i\}$ generated by Algorithm 1. Then the following hold:

- (i) For any subsequence $\{\widehat{X}^{i_t}\}_t$ such that $\widehat{X}^{i_t} \rightarrow X^*$ for some optimal solution X^* of (CVX), $X^{i_t} \rightarrow X^*$ as well.
- (ii) For the same subsequence as above, if X^* satisfies the nondegeneracy condition

$$0 \in \text{relint}(\partial F(X^*)) ,$$

then there is $t_0 \geq 0$ such that $\text{rank}(X^{i_t+1}) = \text{rank}(X^*)$ for all $t \geq t_0$.

3.5 Dual Variable Recovery

After solving the ALM subproblem (CVX), we obtain a primal solution X . To verify that X satisfies the KKT conditions of both the ALM subproblem (CVX) and the original problem (SDP), it is necessary to recover the remaining dual variables. While the ALM framework already recovers the dual variables y and W , we still need to recover the remaining dual variables U (for $AX = 0$) and S (for $X \succeq 0$). In [15], a recovery procedure based on the low-rank factorization was proposed, but it can suffer from singularity issues and produce an inaccurate dual solution. In [16], an approximate recovery via a PG step was described, which in turn requires solving a nearest-correlation-matrix subproblem using the semismooth Newton-CG method.

By contrast, we present a direct and efficient recovery scheme tailored to (SDP), which (i) avoids any nonsmooth issue, and (ii) requires only a single projection onto the null space of A . Specifically, the KKT system for (CVX) can be written as

$$\begin{aligned} AX = 0, \quad \nabla\phi(X) - A^\top U - U^\top A &= S, \\ \langle X, S \rangle = 0, \quad X \succeq 0, \quad S \succeq 0, \end{aligned} \tag{25}$$

The following theorem shows how to recover the dual variables (U, S) explicitly from X , without solving any large linear system.

Theorem 4. Assume that (CVX) admits an optimal solution satisfying the KKT conditions (25). A matrix $X \in \mathcal{F} \cap \mathbb{S}_+^n$ is a minimizer of (CVX) if and only if

$$\widehat{S} := J(\nabla\phi(X))J \succeq 0 \tag{26}$$

$$X\widehat{S} = 0 \tag{27}$$

where $J := I - A^\top(AA^\top)^{-1}A$ is the orthogonal projector onto the null space of A .

Proof. (1) Suppose (CVX) admits an optimal solution X that satisfies the KKT conditions (25). Then we have:

$$\widehat{S} := J(\nabla\phi(X))J = J(\nabla\phi(X) - A^\top U - U^\top A)J = JSJ \succeq 0,$$

where the second equality follows from $JA^\top = 0$, thus confirming (26). Moreover, since $X \succeq 0$ and $S \succeq 0$, we may write $X = RR^\top$ and $S = VV^\top$ for some matrices R and V . From $\langle X, S \rangle = 0$, it follows that

$$\langle RR^\top, VV^\top \rangle = \|V^\top R\|_F^2 = 0,$$

which implies $XS = RR^\top VV^\top = 0$. Therefore,

$$X\hat{S} = XJSJ = XSJ = 0,$$

where the second equality follows from $XA^\top = 0$. Thus, (27) is satisfied.

(2) Conversely, suppose (26), (27) hold. Define

$$V := (AA^\top)^{-1}A(\nabla\phi(X))\left(I - \frac{1}{2}A^\top(AA^\top)^{-1}A\right).$$

Then we have

$$S := \nabla\phi(X) - A^\top V - V^\top A = J(\nabla\phi(X))J = \hat{S} \succeq 0.$$

Moreover, since $X\hat{S} = 0$, we have $\langle X, S \rangle = \text{Tr}(XS) = \text{Tr}(X\hat{S}) = 0$. Therefore, the KKT conditions (25) are satisfied. \blacksquare

Remark 5. *The theorem further implies that for any SDP problem exhibiting facial structure, there must exist at least one KKT point at which the strict complementarity condition does not hold.*

Remark 6. *Typically, verifying global optimality of an SDP requires solving a linear system of size mn to recover all mn dual variables. In contrast, our recovery strategy involves computing and storing the projector $J = (AA^\top)^{-1}A$ only once, after which it can be efficiently applied to $\nabla\phi(X)$. This leads to a numerically stable, closed-form recovery of (U, S) , significantly simplifying the global-optimality verification process.*

3.6 Efficient projection

When reformulating (P) into (SDP), we must enforce the monomial-consistency constraints ($X \in \mathcal{L}^{\mathcal{A}}$), the polyhedral constraints ($X \in \mathcal{P}^{\mathcal{A}}$), and the normalization constraint ($\langle H^0, X \rangle = 1$). In this subsection, we focus specifically on the case where $\mathcal{P}^{\mathcal{A}} = \mathcal{N}^{\mathcal{A}}$ imposes componentwise nonnegativity. We define the affine subspace

$$\tilde{\mathcal{L}}^{\mathcal{A}} := \mathcal{L}^{\mathcal{A}} \cap \{X \in \mathbb{S}^{\mathcal{A}} \mid \langle H^0, X \rangle = 1\}.$$

Rather than incorporating all constraints directly into the linear system $\mathcal{Q}(X) = b$, which would substantially increase the number of constraints, we instead aggregate them into a single feasibility set:

$$\mathcal{P} := \tilde{\mathcal{L}}^{\mathcal{A}} \cap \mathcal{N}^{\mathcal{A}}.$$

This formulation allows us to enforce all constraints through a single projection onto \mathcal{P} . However, since $\tilde{\mathcal{L}}^{\mathcal{A}}$ involves $\Omega(n^{2\tau})$ constraints and $\mathcal{N}^{\mathcal{A}}$ involve $\Omega(n^{2\tau})$ inequality constraints, a naive projection $\Pi_{\mathcal{P}}(X)$ requires $\mathcal{O}(n^{7\tau})$ time, which is computationally prohibitive for large n or τ .

To overcome this computational bottleneck, we now show that the projection onto \mathcal{P} can in fact be computed efficiently in $\mathcal{O}(n^{2\tau})$ time. The key observation is that the projection onto $\mathcal{P} = \tilde{\mathcal{L}}^{\mathcal{A}} \cap \mathcal{N}^{\mathcal{A}}$ admits a decomposition into sequential projections:

Lemma 2. *The projection onto the intersection $\mathcal{P} = \tilde{\mathcal{L}}^{\mathcal{A}} \cap \mathcal{N}^{\mathcal{A}}$ satisfies*

$$\Pi_{\mathcal{P}} = \Pi_{\mathcal{N}^{\mathcal{A}}} \circ \Pi_{\tilde{\mathcal{L}}^{\mathcal{A}}}. \quad (28)$$

Proof. Partition the index set $\mathcal{A} \times \mathcal{A}$ into blocks

$$B_{\gamma} := \{(\alpha, \beta) \in \mathcal{A} \times \mathcal{A} \mid \alpha + \beta = \gamma\},$$

so that each block B_{γ} consists of pairs (α, β) summing to the same monomial exponent γ . The subspace $\tilde{\mathcal{L}}^{\mathcal{A}}$ enforces equality among entries within each block, and the cone $\mathcal{N}^{\mathcal{A}}$ enforces nonnegativity componentwise. Therefore, the projection onto \mathcal{P} decouples across blocks.

Let $\gamma_0 = (e_1^{\tau}, e_1^{\tau})$ be the unique multi-index where H^0 has support. The normalization constraint $\langle H^0, X \rangle = 1$ in $\tilde{\mathcal{L}}^{\mathcal{A}}$ implies

$$\Pi_{\mathcal{P}}(X)|_{B_{\gamma_0}} = 1 = (\Pi_{\mathcal{N}^{\mathcal{A}}} \circ \Pi_{\tilde{\mathcal{L}}^{\mathcal{A}}})(X)|_{B_{\gamma_0}}.$$

For $\gamma \neq \gamma_0$, the blockwise projection has the closed-form:

$$\Pi_{\mathcal{P}}(X)|_{B_{\gamma}} = \arg \min_{x \geq 0} \sum_{i \in B_{\gamma}} (x - X_i)^2 = \max \left\{ \frac{1}{|B_{\gamma}|} \sum_{i \in B_{\gamma}} X_i, 0 \right\} = (\Pi_{\mathcal{N}^{\mathcal{A}}} \circ \Pi_{\tilde{\mathcal{L}}^{\mathcal{A}}})(X)|_{B_{\gamma}}.$$

Since this holds for every block, the identity (28) follows. ■

By Lemma 2, the projection onto $\mathcal{P}^{\mathcal{A}}$ can be computed efficiently by performing sequential projections onto $\tilde{\mathcal{L}}^{\mathcal{A}}$ and $\mathcal{N}^{\mathcal{A}}$. The projection onto $\mathcal{N}^{\mathcal{A}}$ is simply an entrywise maximum with zero and thus costs $\mathcal{O}(n^{2\tau})$. The naive projection onto $\tilde{\mathcal{L}}^{\mathcal{A}}$ is given by

$$\Pi_{\tilde{\mathcal{L}}^{\mathcal{A}}}(X) = \left(I - \tilde{\mathcal{A}}^* (\tilde{\mathcal{A}} \tilde{\mathcal{A}}^*)^{-1} \right) (\tilde{\mathcal{A}}(X) - \tilde{b}),$$

where $\tilde{\mathcal{A}}(X) = \tilde{b}$ encodes the linear equalities defining $\tilde{\mathcal{L}}^{\mathcal{A}}$. Since there are $\Omega(n^{2\tau})$ such equalities, directly factorizing $\tilde{\mathcal{A}} \tilde{\mathcal{A}}^*$ incurs a cost of $\mathcal{O}(n^{6\tau})$, which is again computationally impractical for large-scale instances.

Instead, the structure revealed in the proof of Lemma 2 offers a more efficient alternative: the projection onto $\tilde{\mathcal{L}}^{\mathcal{A}}$ reduces to computing the arithmetic mean over each block B_{γ} , and fixing all entries in the block B_{γ_0} to one due to the normalization constraint. Since there are at most $\mathcal{O}(n^{2\tau})$ distinct index sums γ , this averaging step requires only $\mathcal{O}(n^{2\tau})$ operations. After this projection, all entries corresponding to the same monomial automatically coincide, satisfying the monomial-consistency requirement. In practice, this averaging is implemented using matrix-based operations that group and update entries with the same index sum. The procedure can be further accelerated by exploiting parallel computation or sparse data structures when appropriate.

4 Extension of RiNNAL-POP for solving moment-SOS relaxation problems

RiNNAL-POP, presented in the last section, is designed to solve the polyhedral-SDP relaxation (P) of the polynomial optimization problem (POP). However, the framework can be extended to handle the moment-SOS relaxation (8) of the general POP formulation (6). In this section, we discuss how such an extension can be achieved.

As mentioned in Subsection 2.3, facial constraints naturally arise in moment-SOS relaxations. We specifically exploit this structure in the algorithm design and consider solving the following general τ th-order moment-SOS relaxation of (6):

$$\min \left\{ \langle Q^0, X \rangle \mid \begin{array}{l} \langle H^0, X \rangle = 1, AX = 0, \langle Q^i, X \rangle = 0, i \in [m], \\ \mathcal{M}_{h_j}(X) \succeq 0, j \in [p], X \in \mathbb{S}_+^{\mathcal{A}_\tau} \cap \mathcal{L}^{\mathcal{A}_\tau} \end{array} \right\}. \quad (29)$$

This problem can be compactly written as

$$\min \left\{ \langle Q^0, X \rangle \mid \mathcal{Q}(X) = 0, \mathcal{M}_{h_j}(X) \in \mathcal{K}^{(j)}, j \in [p], X \in \mathcal{F} \cap \mathcal{P} \cap \mathcal{K} \right\}, \quad (30)$$

where $\mathcal{K} := \mathbb{S}_+^{\mathcal{A}_\tau}$ and $\mathcal{K}^{(j)} := \mathbb{S}_+^{\mathcal{A}_{\tau-1}^{h_j}}$, $\mathcal{Q}(X) := [\langle Q^1, X \rangle, \dots, \langle Q^m, X \rangle]^\top$ and

$$\mathcal{F} := \{X \in \mathbb{S}^{\mathcal{A}_\tau} \mid AX = 0\}, \quad \mathcal{P} := \{X \in \mathcal{L}^{\mathcal{A}_\tau} \mid \langle H^0, X \rangle = 1\}.$$

To apply the augmented Lagrangian framework, we introduce auxiliary variables $Y \in \mathcal{K}$ and $Y^{(j)} \in \mathcal{K}^{(j)}$ for $j \in [p]$, and reformulate (30) into the equivalent splitting form below:

$$\min \left\{ \langle Q^0, X \rangle + \delta_{\mathcal{F} \cap \mathcal{K}}(X) + \delta_{\mathcal{P}}(Y) + \sum_{j=1}^p \delta_{\mathcal{K}^{(j)}}(Y^{(j)}) \mid \begin{array}{l} \mathcal{Q}(X) = 0, X - Y = 0, \\ \mathcal{M}_{h_j}(X) - Y^{(j)} = 0, j \in [p] \end{array} \right\}. \quad (31)$$

RiNNAL-POP can then be extended to solve problem (31) via the augmented Lagrangian method. The corresponding augmented Lagrangian function is given by

$$\begin{aligned} L_\sigma(X, Y, \{Y^{(j)}\}; y, W, \{W^{(j)}\}) := & \langle Q^0, X \rangle + \frac{\sigma}{2} \|\mathcal{Q}(X) - \sigma^{-1}y\|^2 + \frac{\sigma}{2} \|X - Y - \sigma^{-1}W\|^2 \\ & + \frac{\sigma}{2} \sum_{j=1}^p \|\mathcal{M}_{h_j}(X) - Y^{(j)} - \sigma^{-1}W^{(j)}\|^2 - \frac{1}{2\sigma} \|y\|^2 - \frac{1}{2\sigma} \|W\|^2 - \frac{1}{2\sigma} \sum_{j=1}^p \|W^{(j)}\|^2. \end{aligned}$$

Given the initial penalty parameter $\sigma_0 > 0$, dual variable $y_0 \in \mathbb{R}^d$, $W_0 \in \mathcal{K}$ and $W_0^{(j)} \in \mathcal{K}^{(j)}$, the augmented Lagrangian method performs the following steps at the $(k+1)$ -th iteration:

$$\begin{aligned} (X_{k+1}, Y_{k+1}, \{Y_{k+1}^{(j)}\}) = & \operatorname{argmin} \left\{ L_{\sigma_k}(X, Y, \{Y^{(j)}\}; y_k, W_k, \{W_k^{(j)}\}) \mid \begin{array}{l} X \in \mathcal{F} \cap \mathcal{K}, Y \in \mathcal{P}, \\ Y^{(j)} \in \mathcal{K}^{(j)}, j \in [p] \end{array} \right\}, \\ y_{k+1} = & y_k - \sigma_k \mathcal{Q}(X_{k+1}), \\ W_{k+1} = & W_k - \sigma_k (X_{k+1} - Y_{k+1}), \\ W_{k+1}^{(j)} = & W_k^{(j)} - \sigma_k (\mathcal{M}_{h_j}(X_{k+1}) - Y_{k+1}^{(j)}), \quad j \in [p], \end{aligned}$$

where $\sigma_k \uparrow \sigma_\infty \leq +\infty$ are positive penalty parameters. Let $\tilde{y}, \tilde{W} \in \mathbb{S}^n$ and $\tilde{W}^{(k)}$ be fixed. The ALM primal subproblem can be expressed as:

$$\min \left\{ L_\sigma(X, Y, \{Y^{(j)}\}; \tilde{y}, \tilde{W}, \{\tilde{W}^{(k)}\}) \mid X \in \mathcal{F} \cap \mathcal{K}, Y \in \mathcal{P}, Y^{(j)} \in \mathcal{K}^{(j)}, j \in [p] \right\}. \quad (32)$$

In (32), we can first minimize with respective to $Y \in \mathcal{P}$ and $Y^{(j)} \in \mathcal{K}^{(j)}$ to get the following convex optimization problem related only to X :

$$\min \left\{ \begin{array}{l} \phi(X) := \langle C, X \rangle + \frac{\sigma}{2} \|\sigma^{-1} \tilde{y} - (\mathcal{Q}(X) - b)\|^2 \\ \quad + \frac{\sigma}{2} \|X - \sigma^{-1} \tilde{W} - \Pi_{\mathcal{P}}(X - \sigma^{-1} \tilde{W})\|^2 \\ \quad + \frac{\sigma}{2} \sum_{j=1}^p \|\Pi_{\mathcal{K}^{(j)}}(\sigma^{-1} \tilde{W}^{(j)} - \mathcal{M}_{h_j}(X))\|^2 \end{array} \mid X \in \mathcal{F} \cap \mathcal{K} \right\}, \quad (33)$$

where we used the Moreau decomposition theorem in [28], which states that $X = \Pi_{\mathcal{C}}(X) - \Pi_{\mathcal{C}^*}(-X)$ for any closed convex cone \mathcal{C} . Once we obtain the optimal solution \tilde{X} of (33), we can recover the optimal solution $\tilde{Y} = \Pi_{\mathcal{P}}(\tilde{X} - \sigma^{-1} \tilde{W})$ and $\tilde{Y}^{(j)} = \Pi_{\mathcal{K}^{(j)}}(\mathcal{M}_{h_j}(\tilde{X}) - \sigma^{-1} \tilde{W}^{(j)})$.

From here, we can apply the same techniques for solving (CVX) in Section 3 to solve the reduced subproblem (33).

5 Numerical experiments

In this section, we conduct numerical experiments to illustrate the effectiveness of RiNNAL-POP for solving polyhedral-SDP relaxation problems of the form (SDP). All experiments are performed using MATLAB R2023b on a workstation equipped with Intel Xeon E5-2680 (v3) processors and 96GB of RAM.

Baseline Solvers. We compare RiNNAL-POP with SDPNAL+ [38, 45, 46]. While other ALM-based and low-rank SDP solvers exist, we do not include them in our comparison, as they are either incompatible with (SDP) or are clearly outperformed by SDPNAL+ in preliminary tests.

Stopping Conditions. Based on the KKT conditions (14) for (SDP), we define the following relative KKT residuals to assess the accuracy of the solution:

$$R_p := \max \left\{ \frac{\|\mathcal{Q}(X) - b\|}{1 + \|b\|}, \frac{\|X - Y\|}{1 + \|X\| + \|Y\|} \right\}, \quad R_d := \frac{\|\Pi_{\mathbb{S}_+^{n+1}}(S)\|}{1 + \|S\|}, \quad R_c := \frac{|\langle X, S \rangle|}{1 + \|X\| + \|S\|}.$$

We omit residuals associated with the constraints $X \in \mathcal{F} \cap \mathbb{S}_+^{n+1}$, $Y \in \mathcal{P}$, and $W \in N_{\mathcal{P}}(Y)$, as the first is inherently satisfied by the low-rank factorization of X , while the latter two are automatically satisfied by the design of the ALM iteration. For a given tolerance $\text{tol} > 0$, RiNNAL-POP terminates when the maximum residual satisfies $R_{\max} := \max\{R_p, R_d, R_c\} < \text{tol}$ or the maximum time limit `TimeLimit` is reached. In our experiments, we set $\text{tol} = 10^{-6}$ and `TimeLimit = 3600(secs)` for all solvers.

Implementation. In RiNNAL-POP, each augmented Lagrangian subproblem is approximately solved by using a two-phase scheme that alternates between a low-rank phase and

a convex-lifting phase. Both phases employ the projected gradient (PG) method, but with different step selection strategies: the low-rank phase uses Barzilai–Borwein step sizes combined with a nonmonotone line search strategy [11, 15, 19, 39], while the convex-lifting phase uses a fixed stepsize of $1/\sigma_k$. The penalty parameter σ_k is initialized at $\sigma_0 = 1$ and updated dynamically: it is doubled if $R_p / \|\nabla f_r(R)\| \geq 10$, and halved otherwise. The initial rank is set to $r_0 = \min\{200, \lceil n/5 \rceil\}$, and the initial point R_0 is selected randomly from the feasible set \mathcal{M}_{r_0} . In each ALM iteration, the low-rank phase performs at most 50 PG iterations, followed by a single PG step in the convex-lifting phase.

Table Notations. We use ‘-’ to indicate that an algorithm did not achieve the required tolerance `tol` within the maximum time limit `TimeLimit`. Results are reported only when the maximum KKT residual is below 10^{-2} . A superscript “†” on the KKT residual indicates that only moderate accuracy was achieved. In the first column, we list the polynomial-problem dimension n , the SDP-problem dimension N , and the number of equality constraints m , respectively. For the column labeled “Iteration” associated with `SDPNAL+`, the first entry denotes the number of outer iterations, the second entry denotes the total number of semismooth Newton inner iterations, and the third indicates the total number of ADMM+ iterations. Similarly, for the column labeled “Iteration” associated with `RiNNAL-POP`, the first entry corresponds to the number of ALM iterations, the second denotes the total number of projected gradient descent iterations in the low-rank phase, and the third reports the total number of convex lifting steps. The column labeled “Rank” indicates the rank of the final iterate, computed using a threshold of 10^{-6} for both `RiNNAL-POP` and `SDPNAL+`. The “Objective” column denotes the value of the objective function, while the total computation time is listed under “Time”. We denote `RiNNAL-POP` by `RPOP` for brevity.

Tested Problems. We summarize below the polynomial-optimization models examined in our experiments, together with their decision-variable dimension n , POP order (Deg), relaxation order (Relax), the form of equalities (Eq), the form of inequalities (Ineq), the presence of nonnegativity constraints (≥ 0), and the observed runtime ratio `SDPNAL+ / RPOP` (Speedup).

Table 1: Summary of tested problem classes.

Problem	n	Deg	Relax	Eq	Ineq	≥ 0	Speedup
(StQP)	1000 – 6000	2	1	Simplex	-	✓	34 – 36
(StQP)	20 – 80	2	2	Simplex	-	✓	3 – 6
(BIQ)	20 – 60	2	2	Binary	-	✓	10 – 25
(MBP)	30 – 60	2	2	Equipartition	-	✓	21 – 30
(MQKP)	20 – 40	2	2	Binary	Knapsack	✓	10 – 30
(BQM)	20 – 80	4	2	-	Ball	-	6 – 16
(KMP)	20 – 60	4	2	Mean–variance	-	✓	200 – 278
(CST)	1000 – 6000	2	1	Simplex	-	✓	18 – 500
(CST)	20 – 60	4	2	Simplex	-	✓	13 – 173
(NSTF)	20 – 80	3, 4	2	Spherical	-	✓	2 – 7

Problem	n	Deg	Relax	Eq	Ineq	≥ 0	Speedup
(NTF)	10 – 25	3, 4	2	Block spherical	-	✓	2 – 10

5.1 Comparison of relaxation quality and solver performance

We compare the relaxation bound quality and computational efficiency of different SDP-based relaxations for the standard quadratic problem:

$$v^* = \min \left\{ x^\top Q x \mid e^\top x = 1, x \in \mathbb{R}_+^n \right\}. \quad (\text{StQP})$$

Specifically, we consider four SDP-based relaxations distinguished by the inclusion of polyhedral (nonnegativity) constraints, RLT constraints, and PSD localizing matrices constraints. These relaxations are summarized in Table 2.

Relaxation	$X \geq 0$	RLT	Localizing PSD	Remarks
Poly-SDP	✓	-	-	Polyhedral SDP relaxation (P)
Poly-SDP-RLT	✓	✓	-	Add RLT (cf. Figure 3 in Subsection 2.3)
Mom-SOS	-	✓	✓	Moment-SOS relaxation (8)
Poly-Mom-SOS	✓	✓	✓	Add $X \geq 0$

Table 2: Overview of SDP-based relaxations.

The relaxation quality is evaluated using the relative gap:

$$\% \text{gap} = \frac{v^* - v}{\max\{1, |v^*|\}} \times 100\%,$$

where v^* is the optimal value of the StQP and v is the relaxation value. We evaluate both tightness and computational performance on two types of test instances. To ensure a fair comparison, the reported runtimes exclude the time to generate the SDP data and preprocessing for all solvers.

Random instances. We generate random symmetric matrices $Q \in \mathbb{S}^n$ with entries sampled from $\mathcal{N}(0, 1)$, for $n \in \{5, 10, 15, 20\}$. Each relaxation is solved at orders $\tau = 1$ and $\tau = 2$, using RiNNAL-POP (RPOP) with a solver tolerance of $\text{tol} = 10^{-6}$. As the package Gloptipoly [13] is commonly used to solve Mom-SOS relaxations of POPs, for benchmarking purpose, we also report results obtained by using GloptiPoly to solve the Mom-SOS relaxation here with the same tolerance. The resulting relative gaps and computational times are shown in Table 3 and Figure 4. In Figure 4, we omit the results for the second-order Poly-SDP-RLT relaxation, as the first-order relaxation is already tight. We omit the results for the first-order Poly-Mom-SOS relaxation, as it is equivalent to the first-order Poly-SDP-RLT relaxation.

Order	1st	2nd
Poly–SDP	∞	∞
Poly–SDP–RLT	0	0
Mom–SOS	∞	0
Poly–Mom–SOS	0	0

Table 3: Relative gaps (%) of the four relaxations for the random instance.

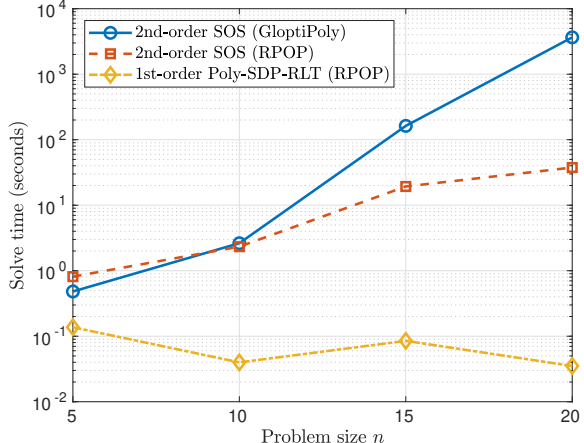


Figure 4: Computational time comparison between GloptiPoly and RPOP.

Extended Horn matrix. For any odd integer $n \geq 5$, Johnson and Reams [20, Section 4] define the matrix $Q_n \in \mathbb{R}^{n \times n}$ by

$$(Q_n)_{ij} = \begin{cases} -1, & |i - j| = 1 \text{ or } \{i, j\} = \{1, n\}, \\ 1, & \text{otherwise,} \end{cases}$$

which is a copositive example with known optimal value $v^* = 0$, attained by any $x = (e_i + e_j)/2$, $1 \leq i < j \leq n$. When $n = 5$, Q_5 coincides with the classical Horn matrix. While many of the tested random instances are tight at first- or second-order relaxation, the extended Horn matrix remains a nontrivial case requiring higher-order relaxations to close the gap. It thus serves as a meaningful benchmark for assessing the strength of different SDP relaxations. For this test, we set $n = 21$ and solve each relaxation at orders $\tau = 1, 2$; in addition, we test GloptiPoly3 for the Mom–SOS relaxation as a benchmark. The resulting gaps and runtimes are reported in Table 4.

Relaxation	1st-order		2nd-order	
	Gap (%)	Time (s)	Gap (%)	Time (s)
Poly–SDP	∞	-	∞	-
Poly–SDP–RLT	0.562	0.3	0.280	4.6
Mom–SOS (RPOP)	∞	-	1.049	1875.4
Mom–SOS (Gloptipoly)	∞	-	1.046	6394.0
Poly–Mom–SOS	0.562	0.3	0.000	245.7

Table 4: Relative gaps and run times for the extended Horn instance ($n = 21$).

The numerical results from both the random and extended Horn instances reveal the following key insights into the relaxation quality and computational performance of different SDP-based relaxations:

1. **RLT and nonnegativity constraints enhance relaxation strength.** Without RLT or nonnegativity constraints, the Poly-SDP and Mom-SOS relaxations remain unbounded at low orders, as evidenced by both the random and extended Horn instances. Incorporating RLT constraints alone (Poly-SDP-RLT) produces finite bounds — it is exact at first order on random matrices and reduces the extended Horn matrix's gap to 0.280% at second order. Even more dramatically, adding nonnegativity constraint to the second order Mom-SOS relaxation (Poly-Mom-SOS) yields an exact bound for the extended Horn example. In contrast, the standard second order Mom-SOS relaxation only achieves a gap of 1.046%.

The above observations show that RLT and nonnegativity constraints complement moment information, closing gaps at lower orders and enhancing both tightness and efficiency. This performance advantage motivates our focus on the Poly-SDP-RLT relaxation in subsequent sections.

2. **Poly-SDP-RLT balances relaxation quality and computational cost.** Among the relaxations tested, Poly-SDP-RLT consistently achieves tight bounds at low computational cost. Remarkably, for the more challenging extended Horn matrix, the first-order Poly-SDP-RLT relaxation can produce a tighter bound than the second-order Mom-SOS relaxation, with a speedup of about 20,000 times. On random instances, Poly-SDP-RLT is exact already at first order. In contrast, Mom-SOS must resort to higher-order moment matrices and incurs substantially longer runtimes. For instance, as shown in Figure 4, at $n = 20$, RPOP solves the first-order Poly-SDP-RLT relaxation about 100,000 times faster than GloptiPoly for solving the second-order Mom-SOS relaxation. This dramatic speedup highlights the efficiency gains from polyhedral strengthening, making Poly-SDP-RLT a scalable and practical alternative to high-order moment-SOS relaxations.
3. **RPOP outperforms GloptiPoly in both efficiency and scalability.** Although originally designed for Poly-SDP-RLT, RPOP extends naturally to moment-SOS problems as we have shown in 4, and it consistently outperforms GloptiPoly across nearly all tested sizes. For example, on random instances with $n = 20$, RPOP solves the second-order Mom-SOS relaxation approximately 100 times faster than GloptiPoly (Figure 4). This performance gap widens with increasing n , reflecting the superior scalability of RPOP's low-rank augmented Lagrangian approach compared to interior-point methods.

5.2 Standard quadratic programming

Consider the following StQP problem mentioned in Subsection 5.1:

$$\min \left\{ x^\top Qx : e^\top x = 1, x \in \mathbb{R}_+^n \right\}. \quad (\text{StQP})$$

To obtain a tractable convex approximation of (StQP), we employ the Poly-SDP-RLT relaxation as detailed in Subsection 5.1. We test on two classes of instances:

1. **Random Gaussian.** For $n \in \{1000, 2000, 4000, 6000\}$, each entry of Q_{ij} is sampled independently from the standard normal distribution $\mathcal{N}(0, 1)$. Empirically, these

matrices often admit extremely sparse solutions x , and the first-order Poly-SDP-RLT relaxation typically yields the exact global optimum.

2. **COP-derived.** For $n \in \{20, 40, 60, 80\}$, we generate Q following the method in [4], which produces instances with a unique minimizer supported on exactly $n/2$ variables. These problems are more challenging, and the first-order relaxation is generally inexact. We therefore apply the second-order Poly-SDP-RLT relaxation, which empirically yields significantly tighter bounds.

The computational results are summarized in Tables 5 and 6.

Table 5: Computational results for StQP problems (relaxation order $\tau = 1$).

(n, N), m	Algorithm	Iteration	Rank	R_{\max}	Objective	Time
(1000,1001) m=1002	RPOP	25, 1238, 25	1	4.32e-07	-4.2604198e-03	15.8
	SDPNAL+	136, 146, 4485	1	4.78e-07	-4.1609498e-03	550.4
(2000,2001) m=2002	RPOP	27, 1400, 27	2	8.66e-07	-2.0202661e-03	100.2
	SDPNAL+	71, 155, 3397	4	4.28e-05 [†]	-2.0064321e-03	3601.3
(4000,4001) m=4002	RPOP	29, 1500, 29	1	5.67e-07	-1.1300123e-03	957.6
	SDPNAL+	12, 30, 400	56	8.35e-05 [†]	-7.3488183e-06	3653.6
(6000,6001) m=6002	RPOP	44, 2250, 44	2	1.99e-05 [†]	-8.3325597e-04	3628.8
	SDPNAL+	0, 0, 117	47	1.75e-03 [†]	-2.7447386e-05	3653.8

As shown in Table 5, RPOP successfully solves all random Gaussian instances to the required accuracy, consistently producing low-rank solutions. On the largest instance ($n = 6000$), although RPOP reaches the time limit, it achieves a KKT residual over 100 times smaller than SDPNAL+, whose solution is both inaccurate and of high rank. Across all tested sizes, RPOP is up to 35 to 40 times faster than SDPNAL+.

Table 6: Computational results for StQP problems (relaxation order $\tau = 2$).

(n, N), m	Algorithm	Iteration	Rank	R_{\max}	Objective	Time
(20,231) m=21022	RPOP	23, 1200, 23	8	3.12e-07	-4.4326119e-02	1.5
	SDPNAL+	0, 0, 338	11	9.43e-07	-4.4340416e-02	4.2
(40,861) m=270642	RPOP	27, 1400, 27	8	8.07e-07	-4.7130297e-02	16.5
	SDPNAL+	0, 0, 422	12	9.48e-07	-4.7150853e-02	65.5
(60,1891) m=1268862	RPOP	24, 1250, 24	8	4.47e-07	-4.8533814e-02	111.8
	SDPNAL+	0, 0, 491	12	9.51e-07	-4.8557752e-02	475.7
(80,3321) m=3855682	RPOP	24, 1250, 24	8	4.14e-07	-4.8304554e-02	623.4
	SDPNAL+	21, 39, 432	21	2.67e-05 [†]	-4.9092914e-02	3604.2

Table 6 presents results for the more challenging COP-derived instances using the second-order Poly-SDP-RLT relaxation. For problem sizes up to $n = 60$, where the lifted SDP already involves tens to hundreds of thousands of constraints due to the RLT and

nonnegativity terms, both solvers reach the required accuracy. However, RPOP consistently yields lower-rank solutions and runs 3 to 4 times faster than SDPNAL+. On the largest instance ($n = 80$), which leads to over 3.8 million linear equality and 11 million nonnegativity constraints, SDPNAL+ fails to reach the required accuracy within the time limit. In contrast, RPOP achieves the required accuracy within 10 minutes, over 6 times faster than SDPNAL+.

5.3 Binary quadratic programs

Consider the following binary quadratic program:

$$\min \left\{ x^\top Qx + c^\top x \mid x \in \{0, 1\}^n \right\}, \quad (34)$$

where $Q \in \mathbb{S}^n$, $c \in \mathbb{R}^n$. This problem can be equivalently reformulated as a polynomial optimization problem in the standard form of (POP) to enable SDP-based relaxation:

$$\min \left\{ x^\top Qx + c^\top x \mid x_i^2 - x_i = 0, \forall i \in [n], x \in \mathbb{R}_+^n \right\}. \quad (\text{BIQ})$$

As demonstrated in [15], the first-order Poly-SDP-RLT relaxation of (BIQ) fails to provide exact bounds. To address this, we apply the second-order Poly-SDP-RLT relaxation, which empirically yields exact bounds across all tested instances, thereby significantly enhancing the relaxation quality. For each $n \in \{20, 40, 60\}$, we generate random instances of (BIQ) by sampling each Q_{ij} and c_i independently from the standard normal distribution $\mathcal{N}(0, 1)$. Each instance is then solved using both RPOP and SDPNAL+, and the results are summarized in Table 7.

Table 7: Computational results for BIQ problems (relaxation order $\tau = 2$).

(n, N), m	Algorithm	Iteration	Rank	R_{\max}	Objective	Time
(20,231) m=20791	RPOP	36, 7332, 8	1	4.43e-07	-4.3222829e+01	5.5
	SDPNAL+	85, 275, 2450		1.36e-07	-4.3222841e+01	55.0
(40,861) m=269781	RPOP	73, 14701, 15	1	1.83e-07	-1.0323647e+02	92.2
	SDPNAL+	186, 1716, 10948		5.85e-07	-1.0323635e+02	2377.0
(60,1891) m=1266971	RPOP	60, 12200, 12	1	3.63e-07	-1.7504234e+02	517.9
	SDPNAL+	28, 236, 1000		2.54e-03 [†]	-1.5375472e+02	3604.0

As shown in Table 7, RPOP solves all instances to the required accuracy and consistently yields rank-one solutions, confirming the empirical tightness of the second-order Poly-SDP-RLT relaxation. In contrast, SDPNAL+ exhibits deteriorating performance as problem size increases. For the medium-scale instance ($n = 40$), RPOP is over 25 times faster. For the largest instance ($n = 60$), RPOP converges within 10 minutes with an accurate, rank-one solution, whereas SDPNAL+ fails to reach the required accuracy within the one-hour time limit and terminates with an approximate solution with poor KKT residual. These results highlight the robustness and efficiency of RPOP in producing low-rank, high-quality solutions for increasingly large-scale Poly-SDP-RLT relaxations of binary quadratic problems.

5.4 Minimum bisection problem

Consider the minimum bisection problem over undirected graphs with n nodes, formulated as the following binary quadratic program:

$$\min \left\{ x^\top L x : e^\top x = \frac{n}{2}, x \in \{0, 1\}^n \right\}, \quad (\text{MBP})$$

where L is the Laplacian of a random Erdos–Renyi graph $G(n, p)$ with edge probability $p = 0.5$, and the equality constraint enforces an equipartition of the vertices. For each $n \in \{30, 40, 50, 60\}$, we generate a single random instance and solve its second-order Poly-SDP-RLT relaxation, since the first-order relaxation fails to provide tight bounds. Table 8 summarizes the performance of RPOP and SDPNAL+.

Table 8: Computational results for MB problems (relaxation order $\tau = 2$).

(n, N), m	Algorithm	Iteration	Rank	R_{\max}	Objective	Time
(30,496) m=107137	RPOP	123, 6200, 25	2	9.38e-09	3.7600000e+02	17.6
	SDPNAL+	45, 235, 2900	2	4.18e-07	3.7599983e+02	365.4
(40,861) m=305082	RPOP	32, 6463, 7	2	7.60e-07	6.3600021e+02	64.2
	SDPNAL+	82, 522, 5233	2	2.23e-07	6.3600002e+02	1878.5
(50,1326) m=697477	RPOP	248, 49800, 50	5	1.22e-07	9.5600001e+02	1014.8
	SDPNAL+	44, 652, 2827	1316	1.24e-03 [†]	9.6287415e+02	3600.6
(60,1891) m=1382322	RPOP	385, 77200, 77	52	3.36e-04 [†]	1.4479773e+03	3606.9
	SDPNAL+	25, 96, 777	1888	4.02e-03 [†]	1.4615768e+03	3600.9

As shown in Table 8, RPOP solves all instances up to $n = 50$ to the required accuracy, while SDPNAL+ fails to reach the target accuracy for $n = 50$, returning a high-rank solution with poor KKT residuals. For $n = 30$ and $n = 40$, RPOP is 20–30 times faster than SDPNAL+. At $n = 60$, neither solver meets the accuracy requirement within the time limit, but RPOP produces a lower-rank solution with a KKT residual that is an order of magnitude smaller than that of SDPNAL+.

5.5 Multiple quadratic knapsack problem

Consider the following multiple quadratic knapsack problem (MQKP) with d knapsacks and n items:

$$\max \left\{ x^\top Q x + c^\top x \mid Ax \leq b, x \in \{0, 1\}^n \right\}, \quad (35)$$

where $Q \in \mathbb{R}^{n \times n}$ is a symmetric profit matrix, $c \in \mathbb{R}^n$ is a linear profit vector, $A \in \mathbb{R}^{d \times n}$ has entries A_{ij} denoting the weight of item j in knapsack i , and $b \in \mathbb{R}^d$ is the capacity vector. To convert the problem into the standard form (POP), we follow the strategy described in Subsection 2.1 by introducing nonnegative slack variables $s \in \mathbb{R}_+^d$ for each capacity constraint, leading to the equivalent reformulation:

$$\max \left\{ x^\top Q x + c^\top x \mid Ax + s = b, x \in \{0, 1\}^n, (x, s) \in \mathbb{R}_+^{n+d} \right\}. \quad (\text{MQKP})$$

We generate test instances using the method described by Gallo et al. [10]. For each problem size $n \in \{10, 20, 30, 40\}$ and knapsack number $d = \{3, 6\}$, we let the probability of a nonzero quadratic interaction be $p = 0.25$ and for each $i < j$ set

$$Q_{jj} = 0, \quad Q_{ij} = Q_{ji} = \begin{cases} 0, & \text{with probability } 1 - p, \\ \text{Uniform}\{1, \dots, 100\}, & \text{with probability } p. \end{cases}$$

We then draw each linear coefficient c_j uniformly from $[1, 100]$ and each weight A_{ij} uniformly from $[1, 50]$. Finally, we set the capacity of knapsack i to $b_i = \lceil 0.1 \sum_{j=1}^n A_{ij} \rceil$. Since the first-order Poly-SDP-RLT relaxation of (MQKP) is not tight, we solve the second-order relaxation using SDPNAL+ and RiNNAL-POP. Numerical results are reported in Table 9.

Table 9: Computational results for MQKP problems (relaxation order $\tau = 2$).

(n, N, d), m	Algorithm	Iteration	Rank	R_{\max}	Objective	Time
(20,300,3) m=55201	RPOP SDPNAL+	28, 5800, 28 18, 86, 500	1 1	8.74e-08 1.25e-07	-2.1400018e+02 -2.1400000e+02	7.6 88.3
(20,378,6) m=113023	RPOP SDPNAL+	26, 5400, 26 12, 42, 350	1 1	7.80e-07 8.63e-08	-1.6800001e+02 -1.6800000e+02	10.0 101.3
(30,595,3) m=189806	RPOP SDPNAL+	34, 7000, 34 34, 177, 2100	1 1	3.19e-07 1.06e-07	-7.8400063e+02 -7.8400003e+02	29.0 900.6
(30,703,6) m=333223	RPOP SDPNAL+	90, 18200, 90 54, 250, 3700	2 1	4.54e-07 1.28e-08	-3.9600026e+02 -3.9600000e+02	114.8 2958.7
(40,990,3) m=482461	RPOP SDPNAL+	100, 20200, 100 46, 252, 2900	4 12	8.16e-07 5.96e-05 [†]	-1.1970070e+03 -1.1969960e+03	223.4 3639.2
(40,1128,6) m=769673	RPOP SDPNAL+	848, 169800, 848 25, 113, 1300	237 469	2.43e-04 [†] 1.45e-03 [†]	-9.0042934e+02 -9.2321049e+02	3603.1 3708.0

As shown in Table 9, RPOP consistently solves all instances to the required accuracy, recovering rank-one or nearly rank-one solutions except the last instance. In contrast, SDPNAL+ experiences significant difficulty on the larger instances. For $n \leq 30$, both solvers achieve the required accuracy, but RPOP is 10–30 times faster. On the more challenging instances with $n = 40$, the performance gap widens substantially. For example, for the instance with $d = 3$, RPOP converges within 4 minutes, while SDPNAL+ terminates with a high-rank solution and fails to meet the required accuracy within the 1-hour time limit.

5.6 Ball-constrained quartic minimization

Consider the following quartic minimization problem over the $(n-1)$ -dimensional Euclidean unit ball:

$$\min \left\{ \langle c, [x]_4 \rangle \mid \|x\| \leq 1, x \in \mathbb{R}^{n-1} \right\}, \quad (36)$$

where $[x]_4$ is the vector of monomials in x of degree up to 4, and $c \in \mathbb{R}^\ell$ is a given coefficient vector with $\ell := \binom{n+3}{4}$. To convert the problem into the standard form (POP), we follow

the strategy described in Subsection 2.1 by introducing a squared slack variable $s \in \mathbb{R}$ and equivalently reformulate (36) as a sphere-constrained problem:

$$\min \left\{ \langle c, [x]_4 \rangle \mid \|x\|^2 + s^2 = 1, (x, s) \in \mathbb{R}^n \right\}. \quad (\text{BQM})$$

For each $n \in \{20, 40, 60, 80\}$, we generate random instances by sampling each coefficient $c_i \sim \mathcal{N}(0, 1)$. For this special problem (BQM) with a constraint over the unit sphere, the solver ManiSDP [43] can be used to solve the relaxation problems. We solve the resulting second-order Poly-SDP-RLT relaxation of (BQM) using SDPNAL+, ManiSDP, and RiNNAL-POP, and summarize the numerical results in Table 10.

Table 10: Computational results for BQM problems (relaxation order $\tau = 2$).

(n, N), m	Algorithm	Iteration	Rank	R_{\max}	Objective	Time
(20,231) m=16402	RPOP	25, 520, 25	1	2.65e-07	-1.2346539e+01	0.6
	SDPNAL+	11, 23, 300	1	3.37e-07	-1.2346534e+01	3.5
	ManiSDP	96	1	1.96e-07	-1.2346549e+01	6.8
(40,861) m=236202	RPOP	21, 440, 21	1	5.18e-07	-2.0874267e+01	4.4
	SDPNAL+	6, 27, 623	2	9.80e-07	-2.0874046e+01	72.3
	ManiSDP	180	10	1.35e-02 [†]	-2.1770028e+01	93.2
(60,1891) m=1155402	RPOP	44, 900, 44	1	7.76e-07	-2.2240284e+01	67.1
	SDPNAL+	8, 30, 599	2	9.59e-07	-2.2239502e+01	491.2
	ManiSDP	-	-	-	-	-
(80,3321) m=3590002	RPOP	51, 1040, 51	1	2.04e-07	-2.7585001e+01	372.1
	SDPNAL+	8, 30, 588	2	9.54e-07	-2.7583874e+01	3167.5
	ManiSDP	-	-	-	-	-

As shown in Table 10, both RPOP and SDPNAL+ successfully solve all test instances to the required accuracy, consistently recovering rank-one or low-rank solutions. In contrast, ManiSDP fails to solve problems with $n \geq 40$, due to early termination from its stagnation-based stopping criterion. At $n = 40$, RPOP is over 15 times faster than SDPNAL+, and more than 20 times faster than ManiSDP. For larger instances ($n = 60, 80$), RPOP continues to outperform SDPNAL+ with speedups of approximately 7–9 times, while ManiSDP fails to converge. These results demonstrate the scalability and numerical stability of RPOP in solving Poly-SDP-RLT relaxations of dense quartic problems over high-dimensional unit ball.

5.7 Kurtosis-minimization portfolio problem

Consider the kurtosis-minimization portfolio model under fixed expectation and risk levels:

$$\min \left\{ \mathbb{E}_{\xi}[(x^\top (\xi - \mu))^4] \mid \mu^\top x = \mu_0, x^\top \Sigma x = \sigma_0^2, e^\top x = 1, x \geq 0 \right\}, \quad (\text{KMP})$$

where $\xi \in \mathbb{R}^n$ denotes the random asset-return vector, $\mu = \mathbb{E}[\xi] \in \mathbb{R}^n$ its mean vector, $\Sigma = \text{Cov}(\xi) \in \mathbb{R}^{n \times n}$ the covariance matrix, $e \in \mathbb{R}^n$ the all-ones vector, and $x \in \mathbb{R}^n$ the

decision variable representing long-only portfolio weights. The parameters μ_0 and σ_0^2 denote the target expected return and variance, respectively.

Problem (KMP) corresponds to P3 in [26], and we generate synthetic data following the setup in [18]. For each $n \in \{20, 40, 60, 80\}$, we draw $p = 255$ independent asset-price samples $\xi_i \in \mathbb{R}^n$ uniformly from $(0, 10)^n$. Letting $\hat{\mu}$ and $\hat{\Sigma}$ denote the empirical mean and covariance of $\{\xi_i\}_{i=1}^p$, we set

$$\mu_0 = \hat{\mu}^\top \left(\frac{e}{n} \right), \quad \sigma_0^2 = \left(\frac{e}{n} \right)^\top \hat{\Sigma} \left(\frac{e}{n} \right),$$

so that the targets match those of the equally-weighted portfolio $x = e/n$. We solve the second-order Poly-SDP-RLT relaxation using RPOP and SDPNAL+. Table 11 summarizes the results.

Table 11: Computational results for KM problems (relaxation order $\tau = 2$).

(n, N), m	Algorithm	Iteration	Rank	R_{\max}	Objective	Time
(20,231) m=26104	RPOP	14, 750, 14	1	4.81e-07	5.3904621e-01	0.7
	SDPNAL+	85, 405, 3337	1	9.66e-07	5.4569096e-01	194.5
(40,861) m=306804	RPOP	41, 2100, 41	5	6.76e-07	8.0918582e-02	18.9
	SDPNAL+	77, 634, 3650	39	6.24e-06 [†]	9.0307077e-02	3602.7
(60,1891) m=1386104	RPOP	172, 8650, 172	56	9.98e-07	3.0082122e-02	464.3
	SDPNAL+	20, 67, 650	112	1.95e-04 [†]	7.2863598e-02	3626.3
(80,3321) m=4128004	RPOP	139, 7000, 139	74	9.97e-07	1.3900566e-02	1831.2
	SDPNAL+	-	-	-	-	-

As shown in Table 11, RPOP successfully solves all instances to the required accuracy, while SDPNAL+ fails to converge within the 1-hour time limit for instances with $n \geq 40$. At $n = 20$, RPOP is over 270 times faster than SDPNAL+. As the problem size increases, the performance gap widens significantly: for $n = 40$, RPOP converges within 20 seconds, while SDPNAL+ fails to converge within the 1-hour time limit; at $n = 60$, RPOP solves the problem in 8 minutes, whereas SDPNAL+ terminates with a large KKT residual. For $n = 80$, only RPOP is able to solve the instance, as SDPNAL+ encounters memory issues due to over 4 million equality constraints and more than 11 million nonnegativity constraints. The high efficiency of RPOP is partly attributed to the highly structured nature of the relaxation, which introduces numerous facial equality constraints that are effectively exploited in the design of our algorithm.

5.8 Copositivity of symmetric tensors

Let $\mathcal{B} \in \text{Sym}(\otimes^t \mathbb{R}^n)$ be a symmetric tensor of order t . The tensor \mathcal{B} is said to be copositive if

$$\langle \mathcal{B}, \otimes^t x \rangle \geq 0 \quad \text{for all } x \in \mathbb{R}_+^n.$$

When $t = 2$, this definition reduces to the classical notion of matrix copositivity. Testing tensor copositivity for general t is co-NP-hard [8, 29], and can be reformulated as the

polynomial optimization problem

$$\min \left\{ \langle \mathcal{B}, \otimes^t x \rangle \mid e^\top x = 1, x \geq 0 \right\}. \quad (\text{CST})$$

The tensor \mathcal{B} is copositive if and only if the optimal value of (CST) is nonnegative. We consider two types of test instances constructed according to the method described in [33]:

1. **Random symmetric tensors.** Each entry of \mathcal{B} is sampled independently from the uniform distribution on $[-1, 1]$, and full symmetry is enforced by averaging over index permutations.
2. **Guaranteed-copositive tensors.** A sufficient condition for copositivity is that

$$\mathcal{B}_{ii\cdots i} \geq - \sum \left\{ \mathcal{B}_{ii_2\cdots i_t} : (i, i_2, \dots, i_t) \neq (i, i, \dots, i) \text{ and } \mathcal{B}_{ii_2\cdots i_t} < 0 \right\} \quad \forall i = 1, \dots, n.$$

To construct such tensors, we first generate a random symmetric tensor as above. Then, for each $i = 1, \dots, n$, we set

$$\mathcal{B}_{ii\cdots i} = 10^{-6} - \sum \left\{ \mathcal{B}_{ii_2\cdots i_t} : (i, i_2, \dots, i_t) \neq (i, i, \dots, i) \text{ and } \mathcal{B}_{ii_2\cdots i_t} < 0 \right\},$$

which ensures that the copositivity condition is satisfied and \mathcal{B} is copositive by construction.

For matrix instances ($t = 2$), the first-order Poly-SDP-RLT relaxation is already tight. Thus, we test the first-order relaxation with $n \in \{1000, 2000, 4000, 6000\}$. For the fourth-order tensor instances ($t = 4$), the relaxation order must be at least 2 to capture the degree of the polynomial. Accordingly, we apply the second-order Poly-SDP-RLT relaxation with $n \in \{20, 40, 60\}$. The numerical results are summarized in Tables 12 and 13. In these tables, DT denotes the data type.

Table 12: Computational results for CST problems with $t = 2$ (relaxation order $\tau = 1$).

DT	(n, N), m	Algorithm	Iteration	Rank	R_{\max}	Objective	Time
1	(1000,1001) m=1002	RPOP	116, 5843, 116	1	7.96e-07	-9.9221196e-01	38.2
		SDPNAL+	227, 247, 5330	2	1.66e-06 [†]	-9.9184447e-01	702.1
1	(2000,2001) m=2002	RPOP	136, 6850, 136	4	8.86e-07	-9.9850085e-01	300.2
		SDPNAL+	130, 201, 3307	19	1.86e-05 [†]	-9.9420320e-01	3601.3
2	(1000,1001) m=1002	RPOP	2, 80, 2	1	1.74e-14	1.6615831e-01	0.9
		SDPNAL+	45, 45, 2307	1	9.10e-07	1.6799439e-01	221.9
2	(2000,2001) m=2002	RPOP	2, 80, 2	1	5.88e-15	1.6655448e-01	4.2
		SDPNAL+	105, 108, 2723	1	8.54e-07	1.7012510e-01	2107.7
2	(4000,4001) m=4002	RPOP	2, 84, 2	1	2.03e-14	1.6643175e-01	30.9
		SDPNAL+	20, 20, 458	797	1.21e-05 [†]	2.7370011e+00	3605.1
2	(6000,6001) m=6002	RPOP	1, 77, 1	1	7.17e-07	1.6667974e-01	68.1
		SDPNAL+	0, 0, 153	1	5.39e-06 [†]	5.0527070e-01	3613.0

As shown in Table 12, RPOP successfully solves all matrix copositivity instances using the first-order Poly-SDP-RLT relaxation, whereas SDPNAL+ is unable to solve several large-scale or difficult instances within the 1-hour time limit, particularly for data type 2. For these problems, RPOP achieves up to 500 times speedups and consistently delivers low-rank solutions.

Table 13: Computational results for CST problems with $t = 4$ (relaxation order $\tau = 2$).

DT	(n, N), m	Algorithm	Iteration	Rank	R_{\max}	Objective	Time
1	(20,231) m=21022	RPOP	14, 750, 14	2	6.42e-07	-9.4311726e-01	0.7
		SDPNAL+	15, 17, 830		8.50e-07	-9.4292047e-01	9.3
1	(40,861) m=270642	RPOP	30, 1549, 30	1	1.60e-07	-9.6583382e-01	17.6
		SDPNAL+	90, 116, 2694		8.68e-07	-9.6482563e-01	399.8
1	(60,1891) m=1268862	RPOP	54, 2733, 54	1	3.75e-07	-9.9430793e-01	217.5
		SDPNAL+	50, 99, 3226		1.80e-05 [†]	-9.9445335e-01	3601.1
2	(20,231) m=21022	RPOP	18, 950, 18	1	3.35e-07	5.3540264e-02	0.9
		SDPNAL+	83, 599, 3477		1.00e-06	5.3809530e-02	156.3
2	(40,861) m=270642	RPOP	19, 1000, 19	1	7.13e-07	5.0214195e-02	9.4
		SDPNAL+	31, 172, 1001		8.63e-07	5.0348184e-02	514.5
2	(60,1891) m=1268862	RPOP	21, 1100, 21	1	5.27e-07	4.8896302e-02	71.2
		SDPNAL+	18, 103, 322		9.89e-07	1.9684112e+00	2185.9

In the tensor setting (Table 13), RPOP again demonstrates clear superiority. For data type 1, it is typically 10–20 times faster than SDPNAL+, and for data type 2, the speedup reaches 30–150 times. Notably, even when both solvers satisfy the stopping criteria, SDPNAL+ may return objective values with noticeable deviation (e.g., $n = 60$) due to looser complementarity tolerances. With a smaller stopping tolerance, SDPNAL+ would converge to the same value as RPOP. These results highlight RPOP’s efficiency and robustness on copositivity verification tasks for both matrix and higher-order tensor cases.

5.9 Nonnegative tensor factorization

We consider the best nonnegative rank-one approximation of a given tensor. Let

$$\mathcal{B} \in \text{Sym}(\otimes^{\alpha_1} \mathbb{R}^{n_1}) \otimes \cdots \otimes \text{Sym}(\otimes^{\alpha_p} \mathbb{R}^{n_p})$$

be a partially symmetric tensor of order $\sum_{i=1}^p \alpha_i$. The best nonnegative rank-one tensor approximation problem is

$$\min \left\{ \|\mathcal{B} - \lambda x^{\otimes \alpha}\|^2 \mid \|x^{(i)}\| = 1, \lambda \geq 0, x^{(i)} \geq 0, \forall i \in [p] \right\}, \quad (37)$$

where each $x^{(i)} \in \mathbb{R}_+^{n_i}$ has unit Euclidean norm, $\lambda \geq 0$ is a scaling factor, and

$$(x^{(i)})^{\otimes \alpha_i} := \underbrace{x^{(i)} \otimes x^{(i)} \otimes \cdots \otimes x^{(i)}}_{\alpha_i \text{ copies}},$$

so that $x^{\otimes \alpha} = (x^{(1)})^{\otimes \alpha_1} \otimes \cdots \otimes (x^{(p)})^{\otimes \alpha_p}$ is the resulting rank-one tensor. Here $\|\cdot\|$ denotes the Frobenius norm, i.e. $\|\mathcal{T}\|^2 = \sum_{i_1, \dots, i_p} \mathcal{T}_{i_1 \dots i_p}^2$. Eliminating the scalar λ yields the equivalent homogeneous formulation [17]:

$$\min \left\{ \langle -\mathcal{B}, x^{\otimes \alpha} \rangle \mid \|x^{(i)}\| = 1, x^{(i)} \geq 0, \forall i \in [p] \right\}. \quad (\text{NTF})$$

We test two classes of tensors that yield homogeneous polynomial objectives of degree t in the entries of $x^{(i)}$:

1. **General Tensors (NTF).** Set $p = t$, $\alpha_i = 1$, and $n_i = n$ so that $\mathcal{A} \in \otimes^t \mathbb{R}^n$. The entries, given in [30, Example 3.16], are defined as

$$\mathcal{B}_{i_1 \dots i_t} = \sum_{j=1}^t (-1)^{j+1} j e^{-i_j}.$$

2. **Symmetric Tensors (NSTF).** Set $p = 1$, $\alpha_1 = t$, $n_1 = n$, so that $\mathcal{B} \in \text{Sym}(\otimes^t \mathbb{R}^n)$. We test three types of symmetric entries:

$$\mathcal{B}_{i_1 \dots i_t} = \sum_{j=1}^t \frac{(-1)^{i_j}}{i_j}, \quad (\text{NSTF-1})$$

$$\mathcal{B}_{i_1 \dots i_t} = \sum_{j=1}^t \arctan \left(\frac{(-1)^{i_j} i_j}{n} \right), \quad (\text{NSTF-2})$$

$$\mathcal{B}_{i_1 \dots i_t} = \sum_{j=1}^t (-1)^{i_j} \log(i_j). \quad (\text{NSTF-3})$$

These examples are taken from [30, Examples 3.5–3.7].

We test tensors with order $t \in \{3, 4\}$ and apply the second-order Poly-SDP-RLT relaxation to compute lower bounds. Numerical results for the NTF instances are reported in Tables 14 and 15, while results for the NSTF instances are shown in Tables 16 and 17.

Table 14: Computational results for NTF problems with $t = 3$ (relaxation order $\tau = 2$).

(n, N), m	Algorithm	Iteration	Rank	R_{\max}	Objective	Time
(10,496) m=78369	RPOP	25, 1300, 25	4	6.70e-07	-1.1611106e+01	3.4
	SDPNAL+	2, 2, 353	4	8.65e-07	-1.1611100e+01	9.1
(15,1081) m=376189	RPOP	28, 1450, 28	4	7.97e-08	-1.7610440e+01	20.8
	SDPNAL+	11, 11, 694	7	4.41e-07	-1.7610440e+01	87.4
(20,1891) m=1159184	RPOP	27, 1400, 27	4	5.39e-07	-2.3579847e+01	74.4
	SDPNAL+	0, 0, 407	6	9.36e-07	-2.3579808e+01	176.6
(25,2926) m=2788479	RPOP	31, 1600, 31	4	1.30e-07	-2.9535838e+01	362.0
	SDPNAL+	11, 11, 651	9	9.33e-07	-2.9535838e+01	1472.6

As shown in Table 14, both RPOP and SDPNAL+ successfully solve all second-order relaxation problems to the required accuracy. However, RPOP is consistently 3–6 times faster than SDPNAL+.

Table 15: Computational results for NTF problems with $t = 4$ (relaxation order $\tau = 2$).

(n, N), m	Algorithm	Iteration	Rank	R_{\max}	Objective	Time
(10,861) m=238785	RPOP	28, 1450, 28	8	6.40e-07	-3.1637169e+01	12.6
	SDPNAL+	11, 11, 644	8	9.78e-07	-3.1637174e+01	50.3
(15,1891) m=1161075	RPOP	32, 1650, 32	8	5.62e-07	-6.1949211e+01	88.6
	SDPNAL+	13, 13, 1298	17	1.58e-06 [†]	-6.1949379e+01	586.2
(20,3321) m=3599965	RPOP	42, 2150, 42	8	4.28e-07	-9.8202747e+01	632.5
	SDPNAL+	0, 0, 618	12	9.55e-07	-9.8202557e+01	1566.0

As shown in Table 15, both RPOP and SDPNAL+ successfully solve all the instances. However, RPOP consistently achieves a 4–7 times speedup over SDPNAL+.

Table 16: Computational results for NSTF problems with $t = 3$ (relaxation order $\tau = 2$).

NSTF	(n, N), m	Algorithm	Iteration	Rank	R_{\max}	Objective	Time
1	(40,861) m=236202	RPOP	19, 1000, 19	1	2.68e-07	-3.8016921e+01	9.0
		SDPNAL+	0, 0, 331	4	9.75e-07	-3.8016959e+01	25.0
1	(60,1891) m=1155402	RPOP	19, 1000, 19	1	8.35e-07	-5.6213703e+01	54.7
		SDPNAL+	1, 1, 479	1	5.47e-07	-5.6214490e+01	207.0
1	(80,3321) m=3590002	RPOP	29, 1500, 29	2	9.83e-07	-7.4060045e+01	455.1
		SDPNAL+	15, 20, 1000	1	9.16e-07	-7.4060013e+01	3403.3
2	(40,861) m=236202	RPOP	48, 2450, 48	2	3.94e-07	-1.5094742e+02	20.9
		SDPNAL+	22, 25, 650	1	9.58e-07	-1.5094484e+02	76.8
2	(60,1891) m=1155402	RPOP	66, 3350, 66	1	8.90e-07	-2.7343951e+02	179.8
		SDPNAL+	23, 29, 650	1	9.82e-07	-2.7342993e+02	442.9
2	(80,3321) m=3590002	RPOP	61, 3100, 61	1	7.98e-07	-4.1800259e+02	931.1
		SDPNAL+	25, 36, 550	1	8.59e-07	-4.1796967e+02	2431.9
3	(40,861) m=236202	RPOP	46, 2350, 46	1	2.56e-08	-8.6565039e+02	20.2
		SDPNAL+	21, 21, 650	1	5.78e-07	-8.6564524e+02	68.8
3	(60,1891) m=1155402	RPOP	72, 3650, 72	1	2.16e-08	-1.7827863e+03	196.3
		SDPNAL+	22, 24, 650	1	7.91e-07	-1.7827613e+03	398.5
3	(80,3321) m=3590002	RPOP	47, 2400, 47	1	2.57e-08	-2.9604567e+03	720.0
		SDPNAL+	22, 27, 550	1	6.27e-07	-2.9604002e+03	2329.4

Table 16 demonstrates that both RPOP and SDPNAL+ solve all second-order relaxation problems to the required accuracy, producing rank-one or nearly rank-one solutions. RPOP outperforms SDPNAL+ across all test cases, offering 3–5 times speedup on moderate-size instances and up to 7 times on the largest.

Table 17: Computational results for NSTF problems with $t = 4$ (relaxation order $\tau = 2$).

NSTF	(n, N), m	Algorithm	Iteration	Rank	R_{\max}	Objective	Time
1	(40,861) m=236202	RPOP	19, 1000, 19	2	1.99e-07	-2.7517484e+02	8.5
		SDPNAL+	16, 16, 800	3	5.64e-07	-2.7517493e+02	67.0
1	(60,1891) m=1155402	RPOP	18, 950, 18	2	9.42e-07	-4.9982804e+02	50.5
		SDPNAL+	1, 1, 524	2	6.62e-07	-4.9982798e+02	232.7
1	(80,3321) m=3590002	RPOP	28, 1450, 28	2	6.43e-07	-7.6119587e+02	365.0
		SDPNAL+	11, 11, 1142	7	5.72e-06 [†]	-7.6123071e+02	3603.6
2	(40,861) m=236202	RPOP	23, 1200, 23	2	3.65e-07	-1.0807713e+03	10.1
		SDPNAL+	13, 23, 350	2	9.88e-07	-1.0807709e+03	41.0
2	(60,1891) m=1155402	RPOP	21, 1100, 21	2	8.72e-07	-2.3932547e+03	59.7
		SDPNAL+	18, 36, 350	2	8.52e-07	-2.3932470e+03	259.2
2	(80,3321) m=3590002	RPOP	24, 1250, 24	2	5.41e-07	-4.2204249e+03	320.7
		SDPNAL+	23, 46, 550	2	8.67e-07	-4.2204101e+03	2501.8
3	(40,861) m=236202	RPOP	22, 1150, 22	2	1.84e-07	-6.1939590e+03	9.9
		SDPNAL+	3, 3, 350	2	4.75e-07	-6.1939856e+03	33.6
3	(60,1891) m=1155402	RPOP	19, 1000, 19	2	2.66e-07	-1.5592573e+04	54.7
		SDPNAL+	7, 7, 350	2	8.36e-07	-1.5592509e+04	205.1
3	(80,3321) m=3590002	RPOP	15, 800, 15	7	8.53e-07	-2.9869486e+04	207.5
		SDPNAL+	6, 13, 300	2	9.58e-07	-2.9869493e+04	1146.0

As shown in Table 17, RPOP consistently solves all second-order Poly-SDP-RLT relaxations of the NSTF problem, while SDPNAL+ fails for some large-scale instances. RPOP achieves significant speedups over SDPNAL+ across all data types. For small- to medium-scale problems, RPOP is about 3–6 times faster, while for the largest instances ($n = 80$), it can be up to 10 times faster.

6 Conclusions

In this paper, we proposed a unified framework for solving polynomial optimization problems (POPs) via polyhedral-SDP relaxations. We focused primarily on problems with equality and nonnegativity constraints, and showed that general inequality constraints can be equivalently reformulated into this setting using standard or squared slack variables. Within this framework, we established connections and analyzed the relative tightness among various relaxation schemes, including DNN, RLT, and moment-SOS. To efficiently solve the resulting large-scale relaxations, we developed RiNNAL-POP, a low-rank augmented Lagrangian method that alternates between a low-rank phase and a convex lifting phase. The algorithm incorporates two key features that enable scalability and efficiency. First, the large numbers of nonnegativity inequality constraints and consistency equality constraints—both typically of order $\Omega(n^{2\tau})$ —are handled efficiently and jointly through a tailored projection procedure in the convex lifting phase. Second, we identify and exploit the hidden facial structure present in many relaxations and incorporate this into the algo-

rithmic design. In particular, after applying the Burer–Monteiro factorization, we restrict the low-rank subproblems to affine subspaces corresponding to exposed faces of the semidefinite cone, thereby improving numerical stability and computational efficiency. Moreover, our method automatically adjusts the factorization rank, and we provide a theoretical guarantee, via rank identification, that the final rank coincides with that of an optimal solution. Numerical experiments on a variety of test problems demonstrate the robustness and scalability of the proposed method. A natural continuation of the current work is to integrate this framework with relaxation hierarchies to develop efficient global solvers for exactly solving general POPs, particularly those involving nonnegativity constraints.

Acknowledgments

The authors express their gratitude to Professor Ching-pei Lee for his valuable comments on the rank identification results.

References

- [1] N. Arima, S. Kim, and M. Kojima. Further development in convex conic reformulation of geometric nonconvex conic optimization problems. *SIAM Journal on Optimization*, 34(4):3194–3211, 2024.
- [2] S. J. Benson and Y. Ye. Algorithm 875: DSDP5—software for semidefinite programming. *ACM Transactions on Mathematical Software (TOMS)*, 34(3):1–20, 2008.
- [3] A. Berman and N. Shaked-Monderer. *Completely positive matrices*. World Scientific, 2003.
- [4] I. Bomze, B. Peng, Y. Qiu, and E. A. Yildirim. Tighter yet more tractable relaxations and nontrivial instance generation for sparse standard quadratic optimization. *arXiv preprint arXiv:2406.01239*, 2024.
- [5] I. M. Bomze, J. Cheng, P. J. Dickinson, and A. Lisser. A fresh CP look at mixed-binary QPs: new formulations and relaxations. *Mathematical Programming*, 166:159–184, 2017.
- [6] J. M. Borwein and H. Wolkowicz. Facial reduction for a cone-convex programming problem. *Journal of the Australian Mathematical Society*, 30(3):369–380, 1981.
- [7] S. Burer. On the copositive representation of binary and continuous nonconvex quadratic programs. *Mathematical Programming*, 120(2):479–495, 2009.
- [8] P. J. Dickinson and L. Gijben. On the computational complexity of membership problems for the completely positive cone and its dual. *Computational Optimization and Applications*, 57:403–415, 2014.
- [9] D. Drusvyatskiy, H. Wolkowicz, et al. The many faces of degeneracy in conic optimization. *Foundations and Trends® in Optimization*, 3(2):77–170, 2017.

- [10] G. Gallo, P. L. Hammer, and B. Simeone. Quadratic knapsack problems. *Combinatorial Optimization*, pages 132–149, 1980.
- [11] B. Gao, N. T. Son, P.-A. Absil, and T. Stykel. Riemannian optimization on the symplectic Stiefel manifold. *SIAM Journal on Optimization*, 31(2):1546–1575, 2021.
- [12] Q. Han, C. Li, Z. Lin, C. Chen, Q. Deng, D. Ge, H. Liu, and Y. Ye. A low-rank ADMM splitting approach for semidefinite programming. *arXiv preprint arXiv:2403.09133*, 2024.
- [13] D. Henrion, J.-B. Lasserre, and J. Löfberg. GloptiPoly 3: moments, optimization and semidefinite programming. *Optimization Methods & Software*, 24(4-5):761–779, 2009.
- [14] M. R. Hestenes. Multiplier and gradient methods. *Journal of Optimization Theory and Applications*, 4(5):303–320, 1969.
- [15] D. Hou, T. Tang, and K.-C. Toh. A low-rank augmented Lagrangian method for doubly nonnegative relaxations of mixed-binary quadratic programs. *arXiv preprint arXiv:2502.13849*, 2025.
- [16] D. Hou, T. Tang, and K.-C. Toh. RiNNAL+: a Riemannian ALM solver for SDP-RLT relaxations of mixed-binary quadratic programs. *arXiv preprint arXiv:2507.13776*, 2025.
- [17] S. Hu, D. Sun, and K.-C. Toh. Best nonnegative rank-one approximations of tensors. *SIAM Journal on Matrix Analysis and Applications*, 40(4):1527–1554, 2019.
- [18] S. Hu and Q. Wang. A globally convergent method for solving a quartic generalized Markowitz portfolio problem. *Applied Numerical Mathematics*, 179:255–272, 2022.
- [19] B. Iannazzo and M. Porcelli. The Riemannian Barzilai–Borwein method with non-monotone line search and the matrix geometric mean computation. *IMA Journal of Numerical Analysis*, 38(1):495–517, 2018.
- [20] C. Johnson and R. Reams. Constructing copositive matrices from interior matrices. *The Electronic Journal of Linear Algebra*, 17:9–20, 2008.
- [21] S. Kim, M. Kojima, and K.-C. Toh. A geometrical analysis on convex conic reformulations of quadratic and polynomial optimization problems. *SIAM Journal on Optimization*, 30(2):1251–1273, 2020.
- [22] J. B. Lasserre. An explicit exact SDP relaxation for nonlinear 0–1 programs. In *Integer Programming and Combinatorial Optimization: 8th International IPCO Conference, Utrecht, The Netherlands, June 13–15, 2001, Proceedings*, pages 293–303. Springer, 2001.
- [23] J. B. Lasserre. Global optimization with polynomials and the problem of moments. *SIAM Journal on Optimization*, 11(3):796–817, 2001.

- [24] C.-p. Lee, L. Liang, T. Tang, and K.-C. Toh. Accelerating nuclear-norm regularized low-rank matrix optimization through Burer-Monteiro decomposition. *Journal of Machine Learning Research*, 25(379):1–52, 2024.
- [25] A. S. Lewis. Active sets, nonsmoothness, and sensitivity. *SIAM Journal on Optimization*, 13(3):702–725, 2002.
- [26] M. Mhiri and J.-L. Prigent. International portfolio optimization with higher moments. *International Journal of Economics and Finance*, 2(5):157–169, 2010.
- [27] R. D. Monteiro, A. Sujanani, and D. Cifuentes. A low-rank augmented Lagrangian method for large-scale semidefinite programming based on a hybrid convex-nonconvex approach. *arXiv preprint arXiv:2401.12490*, 2024.
- [28] J. J. Moreau. Décomposition orthogonale d'un espace hilbertien selon deux cônes mutuellement polaires. *Comptes rendus hebdomadaires des séances de l'Académie des sciences*, 255:238–240, 1962.
- [29] K. G. Murty and S. N. Kabadi. Some NP-complete problems in quadratic and nonlinear programming. *Mathematical Programming: Series A and B*, 39(2):117–129, 1987.
- [30] J. Nie and L. Wang. Semidefinite relaxations for best rank-1 tensor approximations. *SIAM Journal on Matrix Analysis and Applications*, 35(3):1155–1179, 2014.
- [31] J. Pena, J. C. Vera, and L. F. Zuluaga. Completely positive reformulations for polynomial optimization. *Mathematical Programming*, 151:405–431, 2015.
- [32] M. J. Powell. A method for nonlinear constraints in minimization problems. *Optimization*, pages 283–298, 1969.
- [33] L. Qi. Symmetric nonnegative tensors and copositive tensors. *Linear Algebra and its Applications*, 439(1):228–238, 2013.
- [34] Y. Qiu and E. A. Yıldırım. Polyhedral properties of RLT relaxations of nonconvex quadratic programs and their implications on exact relaxations. *Mathematical Programming*, pages 1–37, 2024.
- [35] R. T. Rockafellar. Augmented Lagrangians and applications of the proximal point algorithm in convex programming. *Mathematics of Operations Research*, 1(2):97–116, 1976.
- [36] H. D. Sherali. RLT: A unified approach for discrete and continuous nonconvex optimization. *Annals of Operations Research*, 149(1):185, 2007.
- [37] J. F. Sturm. Using SeDuMi 1.02, a toolbox for optimization over symmetric cones. *Optimization Methods and Software*, 11(1-4):625–653, 1999.
- [38] D. Sun, K.-C. Toh, Y. Yuan, and X.-Y. Zhao. SDPNAL+: A MATLAB software for semidefinite programming with bound constraints (version 1.0). *Optimization Methods and Software*, 35(1):87–115, 2020.

- [39] T. Tang and K.-C. Toh. A feasible method for general convex low-rank SDP problems. *SIAM Journal on Optimization*, 34(3):2169–2200, 2024.
- [40] T. Tang and K.-C. Toh. A feasible method for solving an SDP relaxation of the quadratic knapsack problem. *Mathematics of Operations Research*, 49(1):19–39, 2024.
- [41] K.-C. Toh, M. J. Todd, and R. H. Tütüncü. SDPT3—a MATLAB software package for semidefinite programming, version 1.3. *Optimization Methods and Software*, 11(1–4):545–581, 1999.
- [42] H. A. Tran and K.-C. Toh. On the convergence rates of moment-SOS hierarchies approximation of truncated moment sequences. *arXiv preprint arXiv:2507.00572*, 2025.
- [43] J. Wang and L. Hu. Solving low-rank semidefinite programs via manifold optimization. *arXiv preprint arXiv:2303.01722v1*, 2023.
- [44] Y. Wang, K. Deng, H. Liu, and Z. Wen. A decomposition augmented Lagrangian method for low-rank semidefinite programming. *SIAM Journal on Optimization*, 33(3):1361–1390, 2023.
- [45] L. Yang, D. Sun, and K.-C. Toh. SDPNAL+: a majorized semismooth Newton-CG augmented Lagrangian method for semidefinite programming with nonnegative constraints. *Mathematical Programming Computation*, 7(3):331–366, 2015.
- [46] X.-Y. Zhao, D. Sun, and K.-C. Toh. A Newton-CG augmented Lagrangian method for semidefinite programming. *SIAM J. Optimization*, 20(4):1737–1765, 2010.

A Examples

Example A.1. Consider the following quadratic optimization problem in the form of (POP):

$$\zeta^* = \min \left\{ f_0(w) \mid f_i(w) = 0, i \in [2], w \in \mathbb{R}_+^3 \right\},$$

where the objective and constraint functions are defined as

$$f_0(w) = w_1^2 + 4w_1 - w_3^2, \quad f_1(w) = (w_2 + w_3 - 1)^2, \quad f_2(w) = (w_1 - 2)^2 + w_2(2w_1 - 3).$$

Take degree $\tau = 1$ and select the monomial basis with its index set

$$\mathcal{A} = \mathcal{A}_1 = \left\{ \begin{bmatrix} 1 \\ 0 \\ 0 \\ 0 \end{bmatrix}, \begin{bmatrix} 0 \\ 1 \\ 0 \\ 0 \end{bmatrix}, \begin{bmatrix} 0 \\ 0 \\ 1 \\ 0 \end{bmatrix}, \begin{bmatrix} 0 \\ 0 \\ 0 \\ 1 \end{bmatrix} \right\}, \quad u^{\mathcal{A}}(x) = x = \begin{bmatrix} x_0 \\ x_1 \\ x_2 \\ x_3 \end{bmatrix} = \begin{bmatrix} 1 \\ w_1 \\ w_2 \\ w_3 \end{bmatrix}.$$

The lifted matrix variable is given by

$$X = u^{\mathcal{A}}(x) u^{\mathcal{A}}(x)^\top = \begin{bmatrix} x_0^2 & x_0x_1 & x_0x_2 & x_0x_3 \\ x_1x_0 & x_1^2 & x_1x_2 & x_1x_3 \\ x_2x_0 & x_2x_1 & x_2^2 & x_2x_3 \\ x_3x_0 & x_3x_1 & x_3x_2 & x_3^2 \end{bmatrix} = \begin{bmatrix} 1 & w_1 & w_2 & w_3 \\ w_1 & w_1^2 & w_1w_2 & w_1w_3 \\ w_2 & w_2w_1 & w_2^2 & w_2w_3 \\ w_3 & w_3w_1 & w_3w_2 & w_3^2 \end{bmatrix}.$$

Since $D = \mathbb{R}_+^3$ is the nonnegative orthant, we obtain the following convex CPP relaxation:

$$\zeta^J = \min \left\{ \langle Q^0, X \rangle \mid X \in J, \langle H^0, X \rangle = 1 \right\}.$$

where $J = \{X \in \text{CPP}^4 \mid \langle Q^i, X \rangle = 0, i = 1, 2\}$, $H^0 \in \mathbb{R}^{4 \times 4}$ has all its entries equal to zero except having the entry one at its $(1, 1)$ position, and

$$Q^0 = \begin{bmatrix} 0 & 2 & 0 & 0 \\ 2 & 1 & 0 & 0 \\ 0 & 0 & 0 & 0 \\ 0 & 0 & 0 & -1 \end{bmatrix}, \quad Q^1 = A^\top A = \begin{bmatrix} -1 \\ 0 \\ 1 \\ 1 \end{bmatrix} \begin{bmatrix} -1 \\ 0 \\ 1 \\ 1 \end{bmatrix}^\top, \quad Q^2 = \begin{bmatrix} 4 & -2 & -3/2 & 0 \\ -2 & 1 & 1 & 0 \\ -3/2 & 1 & 0 & 0 \\ 0 & 0 & 0 & 0 \end{bmatrix}.$$

As shown in [21, Example 4.9], this convex reformulation is exact, i.e., $\zeta^J = \zeta^*$. By taking $\mathcal{P}^A = \mathcal{N}^4$, we obtain the following DNN relaxation:

$$\zeta^{\text{DNN}} = \min \left\{ \langle Q^0, X \rangle \mid \langle H^0, X \rangle = 1, AX = 0, \langle Q^2, X \rangle = 0, X \in \mathbb{S}_+^4 \cap \mathcal{N}^4 \right\},$$

where $\langle Q^1, X \rangle = 0$ is replaced by its equivalent constraint $AX = 0$ (due to the decomposition $Q^1 = A^\top A$ and positive semidefiniteness of X). In this low-order case, the consistency cone \mathcal{L}^A coincides with \mathbb{S}^A and is therefore omitted.